Research article

JGS
*Journal of the Geological Society*

Published Online First

doi:10.1144/jgs2015-163

# Devonian magmatism in the accretionary complex of southern Chile

**F. Hervé[1,2*], M. Calderon[2], C. M. Fanning[3], R. J. Pankhurst[4], F. Fuentes[2], C. W. Rapela[5], J. Correa[1], P. Quezada[1] & C. Marambio[1]**

[1] Departamento de Geología, Universidad de Chile, Plaza Ercilla 803, Santiago, Chile
[2] Carrera de Geología, Universidad Andres Bello, Sazie 2119, Santiago, Chile
[3] Research School of Earth Sciences, Australian National University, Canberra, ACT 0200, Australia
[4] British Geological Survey, Keyworth, Nottingham NG12 5GG, UK
[5] Centro de Investigaciones Geológicas, Universidad Nacional de La Plata-CONICET, La Plata, Argentina
* Correspondence: fherve@cec.uchile.cl

**Abstract:** Supposed or potential Devonian igneous rocks in the accretionary complex of southern Chile were investigated using sensitive high-resolution ion microprobe U–Pb dating of zircon, with Hf- and O-isotope analyses of selected grains. Ages of 384 ± 3 and 382 ± 2 Ma are confirmed for two igneous bodies (another having been previously dated at 397 ± 1 Ma). Detrital zircon ages in the host rocks, some associated with Devonian marine fossils, indicate maximum possible sedimentation ages of *c*. 330 – 385 Ma. Devonian ages of 391 ± 10 and 374 ± 3 Ma for plutonic rocks at the western edge of the North Patagonian Massif are somewhat older than those of orthogneisses in the western flank of the Andes near Chaitén (361 ± 7 and 364 ± 2 Ma). O and Hf isotopes indicate that the Devonian intrusions in the accretionary complex crystallized from mantle-derived magmas, whereas those in the North Patagonian Massif show a strong crustal influence, corresponding to oceanic and continental margin subduction environments of magma genesis, respectively. Devonian zircon provenance in the accretionary complex was from the North Patagonian Massif and not from the mantle-derived intrusions, suggesting that the accretionary complex formed an integral part of the Gondwana margin during Devonian–Carboniferous times.

**Supplementary material:** Description of analytical methods and tables of isotope analytical data are available at http://doi.org/10.6084/m9.figshare.c.2336728.

**Received** 20 March 2015; **revised** 22 December 2015; **accepted** 12 January 2016

Accretionary complexes result from sedimentary, tectonic and metamorphic processes in active continental margins. Some lithologies may be followed for considerable distances along the margin, but the absence of fossils and the polydeformational–polymetamorphic history make it difficult to ascertain whether belts of similar rocks are coetaneous. Increasing knowledge of modern accretionary prisms in the Chilean margin shows that there are some constructive segments, others where no prism is being formed, and some where the prism is being tectonically eroded (Maksymowicz 2015). The Coast Range of south–central Chile is mostly underlain by rocks interpreted as part of a fossil accretionary prism that evolved on the southwestern margin of Gondwana during the late Palaeozoic and early Mesozoic (Fig. 1). This accretionary complex has been divided into a Western Series (a belt consisting of micaschists, metabasites, metacherts and serpentinite, considered to have been basally accreted and metamorphosed under rather high $P/T$ conditions) and an Eastern Series (metapelites and metapsammites, metamorphosed under low $P/T$ conditions), in accordance with the concept of paired metamorphic belts (Miyashiro 1961). Based on sensitive high-resolution ion microprobe (SHRIMP) U–Pb detrital zircon dating of these metasedimentary rocks, Hervé *et al.* (2013) demonstrated large variations in provenance ages for the accretionary complex between 34 and 40°S. Glodny *et al.* (2008) noted that during the late stages of its evolution, the accretionary prism underwent tectonic erosion north of 38°S and accretion to the south.

We have studied rocks intruding, or belonging to, the accretionary complex in southern Chile between *c*. 39 and 43°S (Fig. 2). The area is mostly densely forested with a ground cover of thick soil or Holocene sedimentary and volcanic ash deposits. Diverse rock units of well-defined or supposed Palaeozoic ages have been mapped in this area, although in many cases their mutual relationships and geological evolution are not understood in detail. Only at one locality in the western slope of the main Andean Cordillera (Buil) have fossils of Devonian age been identified (Fortey *et al.* 1992), but the relationship of their unmetamorphosed host rocks to the accretionary complex of the Coast Range remains uncertain.

A petrographical, geochronological and geochemical study of potential Devonian plutons and their host rocks was undertaken with the aim of better defining Devonian geological units and processes. Critical areas were studied in the field and samples were collected (including some from the basement in hydrocarbon exploration boreholes in the Osorno–Llanquihue basin, provided by ENAP (Empresa Nacional del Petróleo)). SHRIMP U–Pb dating of zircon, to determine both the crystallization ages of the intrusive rocks and the maximum possible sedimentation ages and older provenance of the sediments, has been applied systematically in the region for the first time. The first results of this study are given below, with an interpretation of the tectonic setting of emplacement and evolution of the accretionary complex.

## Geological setting

In northern Chile the Devonian has been considered a period of magmatic and metamorphic quiescence (Bahlburg & Hervé 1997), during which a passive continental margin environment was developed. This concept has been extended to central Chile, in part because of the presence of meta-psammopelites not older than Devonian in the Eastern Series (Hervé *et al.* 2013); these were

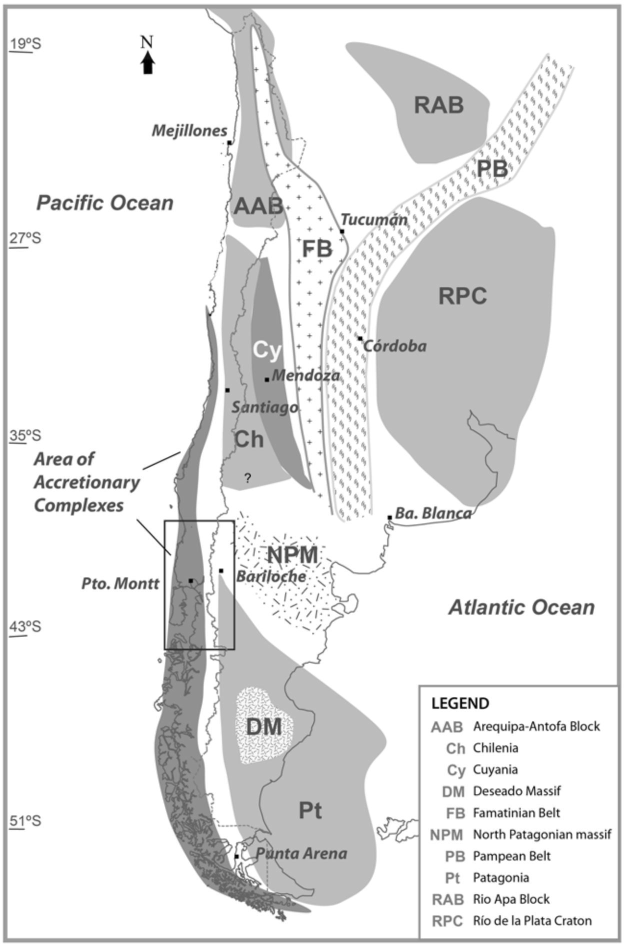


**Fig. 1.** Generalized terrane map of southern South America, modified from Pankhurst *et al.* (2014), with indication of the study area.

interpreted as having been deposited on a passive margin that later became tectonically involved in the accretionary complex. Collision of the Chilenia terrane with Gondwana is considered to have occurred during the Devonian period, through closure of an intervening oceanic basin, the suture being now located in western Argentina (Ramos *et al.* 1986; Cruz Martínez *et al.* 2011; Tomezzoli 2012). The passive margin would have developed at the trailing edge of Chilenia, which probably did not extend farther south than 40°S. Hervé *et al.* (2013) suggested that subduction-related Devonian magmatism occurred south of the area where Chilenia was accreted, as Devonian detrital zircons are found in the Western Series rocks (although many of these rocks are dominated by Permian detrital components). Figure 1 is a general terrane map of southern South America in which the study area is shown in relation to the possible collisions of the Chilenia and Patagonia terranes with the Gondwana margin.

Regional studies (Gonzalez-Bonorino & Aguirre 1970; Aguirre *et al.* 1972; Hervé 1988; Martin *et al.* 1999; Duhart *et al.* 2001; Glodny *et al.* 2005) indicate that psammopelitic schists, greenschists, and minor metachert and serpentinite constitute the basally accreted Western Series of the complex, formed during late Carboniferous to Triassic times. In contrast, the Eastern Series, which at this latitude lies in the western foothills of the main Andean Cordillera, consists of frontally accreted Carboniferous turbiditic successions (Willner *et al.* 2005), formed earlier than the Western Series. From around 39°S to 41°30'S in the study area the Western Series is referred to as the Bahia Mansa metamorphic complex (Duhart 1999), and the Eastern Series as the Trafun metamorphic complex (Campos *et al.* 1998). Isolated outcrops of low-grade metasedimentary rocks, including Early to Middle Devonian fossiliferous slates at Buil (Levi *et al.* 1966; Fortey *et al.* 1992), crop out up to 300 km south of the Trafun metamorphic complex, where they have been considered to form part of the Comau metamorphic complex (Pankhurst *et al.* 1992) and/or the Main Range metamorphic complex (Hervé *et al.* 2003).

The exposed Bahia Mansa metamorphic complex is an assemblage dominated by pelitic to semipelitic schists and subordinate tectonic lenses of quartzose schists of continental derivation. Rocks of oceanic affinity (sheets of mafic schist and minor metachert, and small ultramafic bodies) are tectonically intercalated (Kato 1985; Díaz *et al.* 1988; McDonough *et al.* 1997). Rare earth element geochemistry indicates a normal mid-ocean ridge basalt (N-MORB) protolith for the mafic schists, consistent with the local preservation of pillow structures (Díaz *et al.* 1988; Kato & Godoy 1995; Crignola *et al.* 1997).

## Previous geochronology

Duhart *et al.* (2001) and Duhart (2008) reported U–Pb zircon ages for Devonian igneous rocks. These include (see Fig. 2) the Zarao trachyte (a small igneous body intruding the Western Series in the Coast Range) with a thermal ionization mass spectrometry (TIMS) U–Pb age of 396.7 ± 1.3 Ma, a tonalite intrusion at Pichicolo (SHRIMP, 385 ± 7 Ma) and a coarse-grained metatonalite at Lago Rio Blanco (TIMS, 400 ± 5 Ma and laser ablation inductively coupled plasma mass spectrometry (LA-ICP-MS), 388 ± 6 Ma). There is also an Ar–Ar hornblende age of 359 ± 4 Ma for unexposed granitic rock at the bottom of borehole Rahue-2 in the Cenozoic Osorno–Llanquihue sedimentary basin (M. R. McDonough *et al.*, pers. comm.). Devonian metamorphic ages have been reported for high-grade metabasites in loose boulders at Los Pabilos (Ar–Ar 361 ± 1.7 Ma, Kato *et al.* 2008), and for muscovite from pelitic schists from the bottom of the Los Muermos 2 borehole (K–Ar, 386 ± 9 Ma, M. R. McDonough *et al.*, pers. comm.). McDonough *et al.* considered that the metamorphic and igneous basement rocks of the late Cenozoic Osorno–Llanquihue basin that are reached only in the boreholes belong to a different, older, metamorphic complex, which they named the Llanquihue metamorphic complex. Romero (2014) presented LA-ICP-MS U–Pb ages on detrital zircon from four schists of the Western Series north of Valdivia, which indicate Permian maximum possible sedimentation ages, most with a minor Devonian component.

Finally, a granitoid clast from a conglomerate in the Trafun metamorphic complex at Isla Huapi, Lago Ranco, has been dated at <383 Ma, but was considered to be Devonian (Campos *et al.* 1998).

Interpretation of the geological history of the Bahia Mansa metamorphic complex indicates that $M_1$ high $P/T$ metamorphism in the glaucophane schist and even the eclogite facies occurred before *c.* 361 Ma. $M_2$ low-grade greenschist-facies metamorphism mostly erased the $M_1$ structures and mineral assemblages, and took place during Permian and even Triassic times (Kato *et al.* 1997; Martin *et al.* 1999; Duhart *et al.* 2009).

From the Argentine side of the Andes at these latitudes, Varela *et al.* (2005) reported conventional $^{238}U–^{206}Pb$ zircon ages of 419 ± 27 Ma (MSWD (mean square weighted deviates) = 43) and 390 ± 5 Ma (MSWD = 9) for tonalite near San Martin de los Andes (Fig. 2), and of 348 ± 11 Ma (MSWD = 63) and 387 ± 5 Ma (MSWD = 9) for deformed leucogranite cutting schists. Pankhurst *et al.* (2006) confirmed and refined the age of this magmatism in NW Patagonia with U–Pb zircon SHRIMP ages of 401 ± 3 Ma for the San Martin tonalite and 395 ± 4 Ma for undeformed granite at Lago Lolog about 10 km to the north. They further reported ages of 371 ± 2 Ma for megacrystic granite near Gastre in the southwestern North Patagonian Massif and 394 ± 4 Ma for similar megacrystic granite at Colan Conhue 300 km SE of Bariloche (Fig. 2). Finally, Cruz Martínez *et al.* (2011) reported U–Pb monazite ages (electron probe analyses) of 392 ± 4 and 350 ± 6 Ma for migmatitic gneiss SSW of Bariloche.

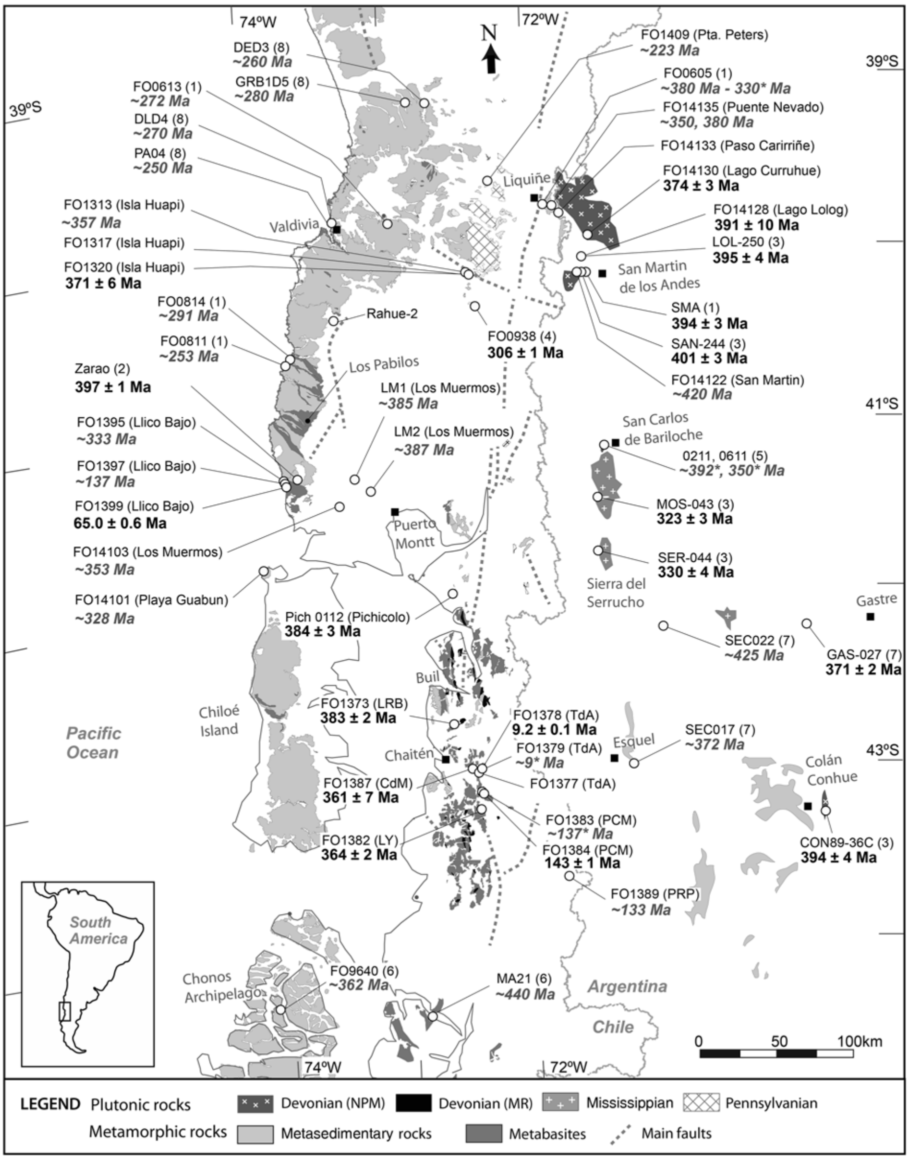


**Fig. 2.** Geological sketch map of the studied portion of the Andes between 39 and 44°S, with location of the rocks dated by U–Pb SHRIMP relevant to this study identified by sample number. LRB, Lago Río Blanco; CdM, Centro del Mundo; LY, Lago Yelcho; TdA, Termas de Amarillo; PCM, Puente Caballo Muerto; PRP, Puente Río Palena. Bold type signifies crystallization ages for igneous rocks and orthogneisses, italic type signifies estimated maximum possible depositional age of metasedimentary protoliths (from minimum age of detrital zircons). Data from this study unless otherwise indicated: 1, Hervé *et al.* (2013); 2, Duhart *et al.* (2001); 3, Pankhurst *et al.* (2006); 4, Deckart *et al.* (2014); 5, monazite Th–Pb ages (Cruz Martínez *et al.* 2011); 6, Hervé *et al.* (2003); 7, Duhart *et al.* (2002); 8, Romero (2014).

## Samples and methods

We have studied more than 200 standard thin sections of rocks, prepared at Universidad de Chile, from the main outcrop areas of the Devonian magmatic rocks and their country rocks. U–Pb SHRIMP analyses of zircon separates from 15 samples were made to determine their igneous crystallization ages. A further 10 separates, mostly from metasedimentary rocks considered initially to be host rocks of the Devonian intrusions, were analysed to study their sedimentary provenance and establish maximum possible sedimentation ages. All samples were collected from localities that display the typical outcrop characteristics of their indicated geological units.

All analytical work was carried out at the Research School of Earth Sciences, the Australian National University, Canberra, using the same U–Pb dating method as given by Hervé *et al.* (2014), whereas the methods for detrital zircon analyses are as given by Hervé *et al.* (2003, 2013). U–Pb SHRIMP analyses using SHRIMP II or SHRIMP RG followed cathodoluminescence (CL) imaging of the zircon grains. Data were processed with SQUID (Ludwig 2009) and Isoplot 3.0 (Ludwig 2003) software. Crystallization ages are reported here with uncertainties at the 95% confidence level. The 2015 IUGS International Chronostratigraphic Chart is used as a reference throughout.

In several of the igneous samples, the U concentrations are high to extreme (see samples FO1320, FO1387 and FO14128). It is well known and documented that SHRIMP analyses of such U-rich areas within zircon grains can give rise to anomalous sputtering of Pb relative to U (Williams & Hergt 2000; White & Ireland 2012). For such areas, the radiogenic $^{206}Pb/^{238}U$ ratios and ages will be anomalous. Williams & Hergt (2000) had contemplated the possibility of a correction factor directly related to the U concentrations, to correct for this anomalous sputtering bias. In practice, no such simple correlation exists (White & Ireland 2012) and so there is no simple solution to the interpretation of Palaeozoic $^{206}Pb/^{238}U$ radiogenic dates for such zircon areas or samples. If the zircon areas all have high to extreme U, the radiogenic $^{207}Pb/^{206}Pb$ ratios and dates can be used to constrain the zircon crystallization age. Unfortunately, where there is a wide range of U concentrations, from low to moderate values (e.g. 100–500 ppm), to high and extreme values greater than, say, 2000 ppm, the $^{207}Pb/^{206}Pb$ ratios and dates are not well constrained for the low- to moderate-U areas. Nevertheless, for such samples we have chosen to use the $^{204}Pb$-corrected $^{207}Pb/^{206}Pb$ ratios and dates as they provide better constraints on the zircon, and enclosing rock, crystallization age.

Single zircon grains were selected for O- and Hf-isotope analyses. SHRIMP U–Pb pits were lightly polished away and oxygen isotope analyses were performed in exactly the same locations using SHRIMP SI (Stable Isotope). Lu–Hf isotopic measurements were carried out by laser ablation multi-collector inductively coupled plasma mass spectrometry (LA-MC-ICP-MS) using a Neptune MC-ICP-MS system coupled with a 193 nm HelEx

**Table 1.** *Summary of U–Pb results for Devonian igneous and metasedimentary rocks*

| Sample number | Location | Geographical coordinates | Lithology | Crystallization age (Ma) |
|---|---|---|---|---|
| *Intrusive bodies* | | | | |
| Pich 0112 | Pichicolo | 41°59.123′S, 72°33.817′W | Hornblende tonalite | 384 ± 3 ($n$ = 20) |
| FO 1373 | Lago Rio Blanco (Chaitén) | 42°44.921′S, 72°36.098′W | Biotite–hornblende tonalite | 383 ± 2 ($n$ = 14) |
| FO1382 | West end of Lago Yelcho | 43°12.658′S, 72°27.058′W | Siliceous gneiss | 364 ± 2 ($n$ = 39) |
| FO1387 | Centro del Mundo quarry | 43°0.341′S, 72°30.605′W | Leucocratic gneiss | 361 ± 7 ($n$ = 23) |
| FO14128 | Lago Lolog | 40°4.253′S, 71°20.073′W | Biotite granodiorite | 391 ± 10 ($n$ = 20) |
| FO14130 | Lago Curruhue Chico | 39°54.722′S, 72°21.027′W | Banded granodiorite | 374 ± 3 ($n$ = 21) |
| **Sample number** | **Location** | **Geographical coordinates** | **Lithology** | **Maximum sedimentation age and peaks (Ma)** |
| *Metasedimentary rocks* | | | | |
| FO1320 | Isla Huapi (Lago Ranco) | 40°14.186′S, 72°23.654′W | Granitic clast | 371 ± 6 ($n$ = 19) |
| FO1313 | Isla Huapi (Lago Ranco) | 40°13.525′S, 72°24.234′W | Metasandstone | 357, 469 |
| LM1 | Drill core, Los Muermos | 41°23.876′S, 73°2.839′W | White mica schist | 385, 411 |
| LM2 | Drill core, Los Muermos | 41°21.426′S, 73°16.478′W | White mica–chlorite schist | 387, 465, 1070 |
| FO1395 | Llico Bajo | 41°11.096′S, 73°42.309′W | White mica schist | 333, 469, 1070 |
| FO14101 | Playa Guabun | 41°49.860′S, 74°1.661′W | White mica schist | 328, 480 |
| FO14103 | Los Muermos | 41°27.640′S, 73°44.375′W | Metasandstone | 353, 366, 380 |
| FO14122 | San Martin de los Andes | 40°10.572′S, 71°23.345′W | Coarse-grained micaschist | 420, 229 |
| FO14135 | Puente Nevado | 39°46.785′S, 71°44.917′W | Biotite–muscovite gneiss | 378, 507, 547 |

ArF Excimer laser. O and Hf isotopic procedures are as given by Hervé *et al.* (2014).

## Geochronological results

### *Igneous intrusions*

Devonian igneous crystallization zircon ages have been obtained for intrusive rocks at Pichicolo and Lago Rio Blanco, for granites from lakes Lolog and Curruhue Chico, as well as for orthogneisses from the Main Range metamorphic complex. In addition, some unexpected post-Palaeozoic ages were obtained from igneous intrusions spatially associated with the accretionary complex and the gneisses; these are presented and discussed in a following section. Results are summarized in Table 1 and presented in Figure 2.

#### *Western slope of the Andes*

Sample Pich 0112, from Pichicolo, is a hornblende tonalite, with mainly poikilitic hornblende phenocrysts dominant over chloritized biotite phenocrysts, in a fine-grained quartz–plagioclase matrix. It is in contact with talc-rich ultramafic rocks according to Duhart *et al.* (2001). The zircon grains are generally subequant euhedral crystals with weakly zoned interiors (Fig. 3a). The areas analysed are dominated by radiogenic Pb and form a simple bell-shaped distribution of $^{206}Pb/^{238}U$ ages, with slight tailing on the older age side attributed to the presence of older zircon components. A weighted mean $^{206}Pb/^{238}U$ age of 384 ± 3 Ma (MSWD = 1.4, 20 analyses; Fig. 4) is interpreted as the time of igneous zircon crystallization, indistinguishable from the SHRIMP age of 385 ± 7 Ma (from only eight grains) presented by Duhart (2008).

A porphyritic leucocratic biotite–amphibole tonalite (FO1373) is exposed in a road cutting near Lago Río Blanco, referred to as the Chaitén metatonalite by Duhart (2008). Plagioclase phenocrysts are embedded in a fine-grained matrix composed of recrystallized quartz, plagioclase, biotite, amphibole, epidote and titanite. Small crystals of biotite form clusters. The tonalite includes a number of septa of foliated and folded metabasites a few metres thick and numerous quartz veins cross-cut the two lithologies. The zircons from the tonalite are complex with a dominant oscillatory-zoned component enclosing older inherited central areas; a few grains have thin, late-stage, high-U rims (Fig. 3b). There is a dominant $^{206}Pb/^{238}U$ age grouping of the oscillatory-zoned areas at *c.* 370–390 Ma, and the probability density plot shows a dominant peak somewhat skewed to younger ages (Fig. 4). There are four younger analyses and these are either of higher U, interpreted as metamict rims (analysis 10.1), or of areas that revealed cracking, which became visible in the post-analysis photographs of spot locations. The four younger analyses are therefore considered to be of areas that have lost radiogenic Pb and the weighted mean $^{206}Pb/^{238}U$ age of 383 ± 2 Ma (MSWD = 1.0, 14 analyses; Fig. 4) gives the dominant time of igneous zircon crystallization. These are all younger than the previous ages obtained by Duhart (2008) (U–Pb TIMS 400 ± 5 Ma, U–Pb LA-ICP-MS 388 ± 6 Ma), although our preferred age of 383 ± 2 Ma is within uncertainty of the LA-ICP-MS date.

Sample FO1382, from the western end of Lago Yelcho, is a quartz-rich rock with anastomosing foliation, composed of quartz, biotite, muscovite and epidote. The zircon grains are characterized by slightly irregular external morphologies developed on primary euhedral crystals. This is better seen under CL imaging (Fig. 3c) where the internal structure is dominated by oscillatory zoning that is cross-cut in many grains by thin unzoned rims and irregularly shaped incursions, interpreted as secondary metamorphic zircon. Three such grains from metamorphic areas have very low Th/U ratios (≤0.04) and yield Cretaceous $^{206}Pb/^{238}U$ ages (*c.* 140 Ma). The zoned igneous component in two of these grains records Devonian–Carboniferous ages (*c.* 368 and *c.* 350 Ma). Three other grains have scattered Permo-Triassic ages, but the vast majority of oscillatory-zoned zircon areas analysed have $^{206}Pb/^{238}U$ ages in the range 350–380 Ma. Areas with slightly younger $^{206}Pb/^{238}U$ ages are considered to have lost radiogenic Pb during formation of the Cretaceous metamorphic overgrowths. A weighted mean $^{206}Pb/^{238}U$ age for 39 out of 66 areas analysed gives 364 ± 2 Ma (MSWD = 1.2; Fig. 4) and this is interpreted as the crystallization age for the oscillatory-zoned, igneous zircon.

FO1387 from the Centro del Mundo quarry is a foliated mylonitic leucocratic gneiss with ribbon quartz, plagioclase, minor hornblende and zircon. It is associated in the field with micaschists and banded amphibolites, in bodies parallel to the foliation. This gneiss belongs to the Main Range metamorphic complex. Euhedral zircon crystals with weakly zoned to oscillatory-zoned interiors predominate (see Fig. 3d). The U concentrations range from low to moderate values (*c.* 60–600 ppm) up to extremely high values (*c.* 6450 ppm). As discussed in the methods section, preference for this dataset is to use the $^{204}Pb$-corrected $^{207}Pb/^{206}Pb$ data and a

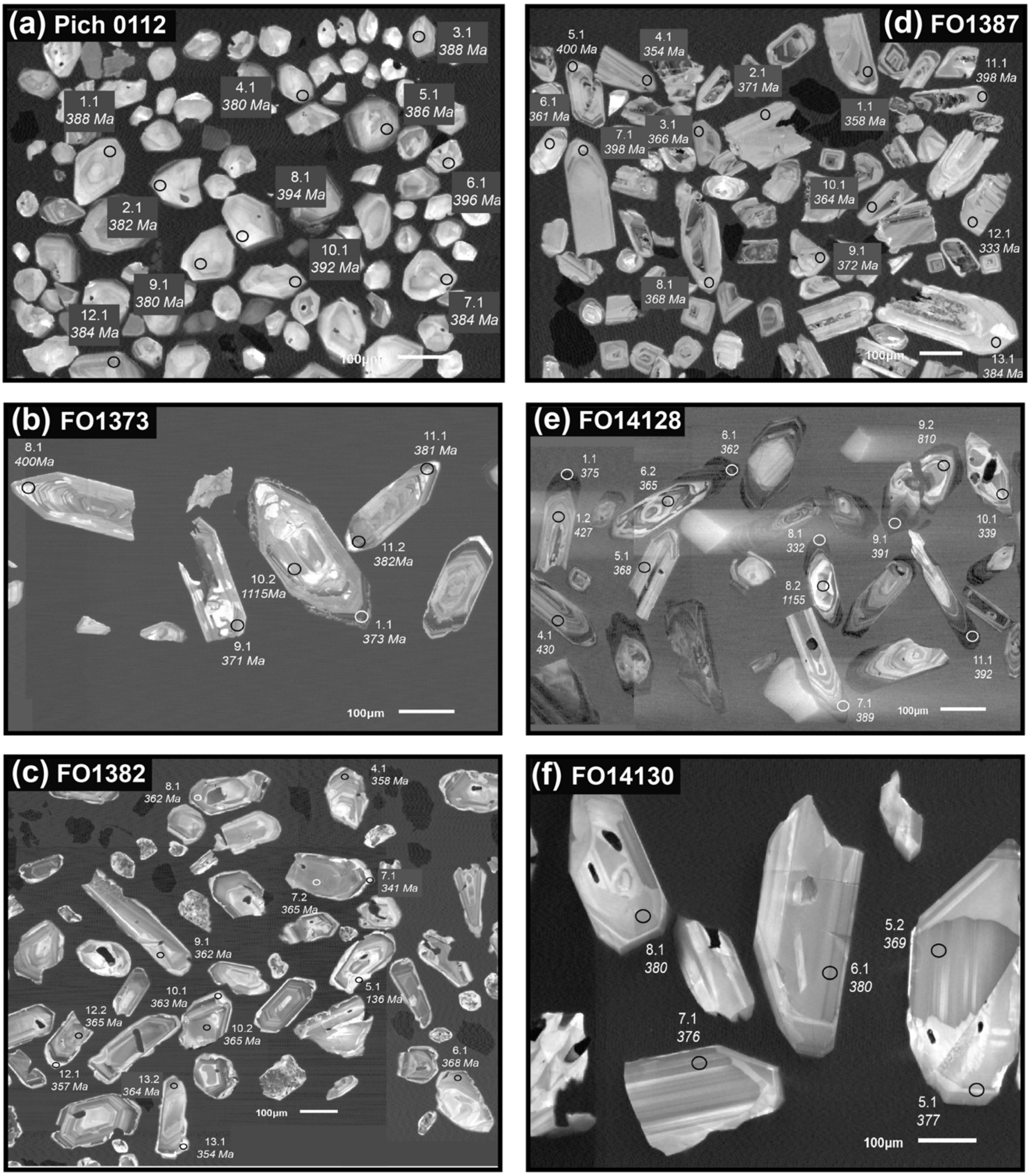


**Fig. 3.** CL images for Devonian igneous intrusions from the study area. Sample numbers and scale indicated in each photograph. Circles indicating the location of areas analysed by SHRIMP are shown in the analysed grains.

Wetherill concordia plot is shown in Figure 5. A regression line fitted to all 23 areas analysed gives an upper intercept of 361 ± 7 Ma (MSWD = 0.82) and this is interpreted to constrain the time of igneous zircon crystallization.

## *North Patagonian massif*

FO14128 is a sample of biotite granodiorite with porphyritic igneous enclaves, from the southern shore of Lago Lolog. A complex variety of internal structures is seen under CL imaging (Fig. 3e). In general, many grains have dark, zoned, high-U outer areas and tips enclosing lower-U central components that are oscillatory-zoned, or have irregular CL features. There is a wide range in U concentrations, from around 120–1220 ppm to at least 5510 ppm. Once again, preference here is to use the $^{204}$Pb-corrected $^{207}$Pb/$^{206}$Pb data and a Wetherill concordia plot is shown in Figure 5. There is dispersion in the $^{206}$Pb/$^{238}$U ratios (and ages) resulting from likely radiogenic Pb loss, coupled with sputtering bias. Excluding the clearly older inherited cores, the analyses define a simple Pb-loss discordia with a poorly constrained upper intercept of 387 ± 23 Ma (MSWD = 1.09, 24 analyses). A weighted mean of the $^{204}$Pb-corrected $^{207}$Pb/$^{206}$Pb ages gives 391 ± 10 Ma (MSWD = 1.2, 20 areas analysed) and this is interpreted as the crystallization age of the zoned magmatic zircon in this sample. A similar array of

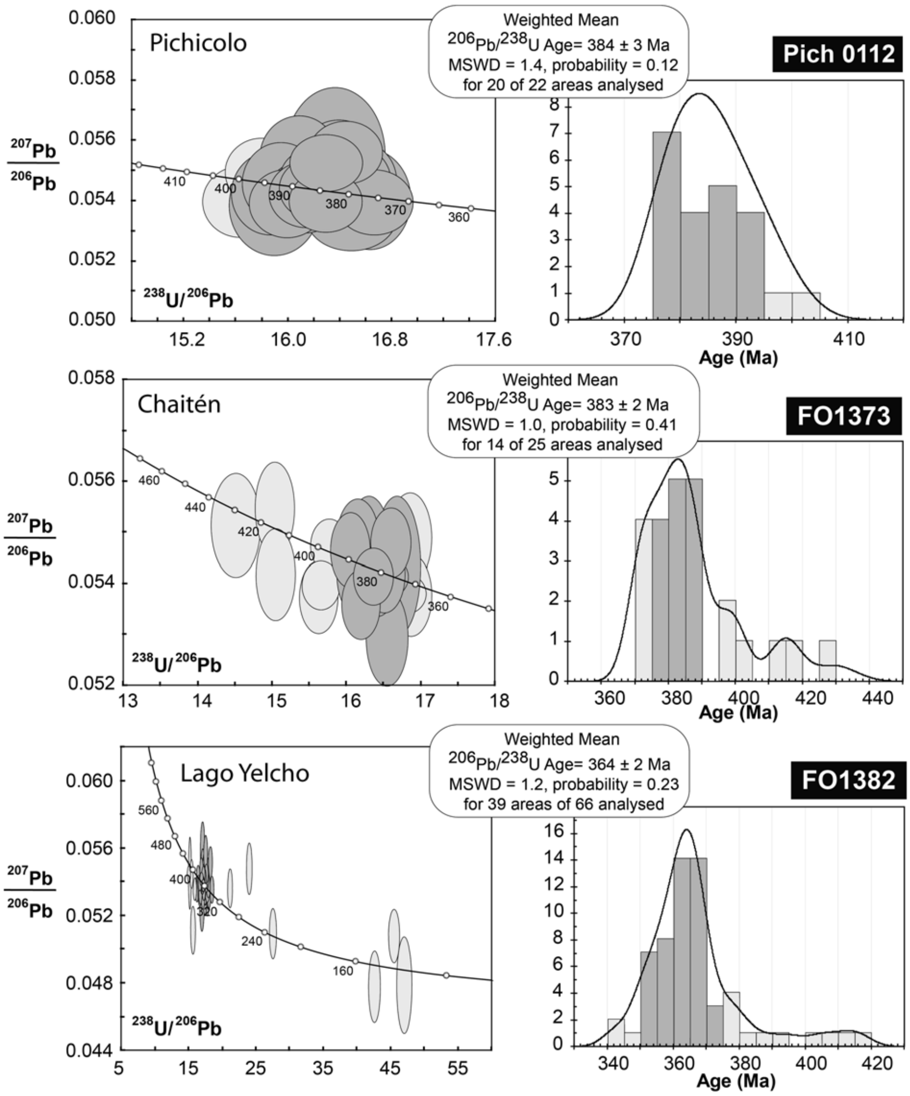


**Fig. 4.** Tera–Wasserburg and age v. probability plots for samples Pich 0112 (Pichicolo tonalite), FO1373 (Chaitén metatonalite at Lago Río Blanco) and FO1382 (Lago Yelcho gneiss). Ellipses represent 68% confidence errors; those in white were excluded from the age calculations in this and all the following similar diagrams.

inheritance and more concordant high-U SHRIMP zircon analyses for the same granite pluton by Pankhurst *et al.* (2006) gave a crystallization age of 395 ± 4 Ma (six analyses).

FO14130 from the western end of Lago Curruhue Chico is a partially banded granodiorite, rich in enclaves of banded gneiss. Vertical and horizontal basic dykes cross-cut this deformed igneous intrusion. The relatively coarse, euhedral, simple igneous zircon (Fig. 3f) analysed from this sample gave a tightly grouped set of $^{206}Pb/^{238}U$ ages with a weighted mean of 374 ± 3 Ma (MSWD = 1.0, all 21 areas analysed, Fig. 5), taken as dating crystallization of the granodiorite.

### *Detrital zircon ages from metasedimentary rocks*

Detrital zircons were dated from metasedimentary rocks of the Trafun metamorphic complex, the Llanquihue basement complex, the Bahia Mansa metamorphic complex, the Main Range metamorphic complex, and the North Patagonian Massif, all of which have given Devonian to Early Carboniferous maximum possible sedimentation ages. Also, a boulder from a diamictite in the Trafun metamorphic complex was dated. Results are summarized in Table 1.

#### *Trafun metamorphic complex*

Included in the renamed Trafun metamorphic complex of Campos *et al.* (1998) is a diamictite at Isla Huapi identified by Thiele *et al.* (1976) and containing granitic clasts, among other lithologies. Martin *et al.* (1999) dated one such clast as probably Devonian (<383 Ma). Correa (2014) collected further samples, data for one of which, FO1320, are reported here. This monzogranite clast has a granular texture with micrographic patches. It consists of a quartz–plagioclase–K-feldspar aggregate, with abundant sericite, calcite, chlorite, epidote and titanite as an alteration assemblage. The zircons are predominantly elongate euhedral grains, many of which are strongly cracked, with metamict areas (Fig. 6): U concentrations show a very wide range (*c.* 75–2880 ppm). Grain 4 yielded an Ordovician $^{206}Pb/^{238}U$ age (*c.* 480 Ma) and is considered an older inherited zircon. As discussed in the methods section, owing to the high U in some of the grains or areas analysed, the $^{204}Pb$-corrected $^{207}Pb/^{206}Pb$ ratios and dates have been preferred for this sample over the more usual $^{207}Pb$-corrected $^{206}Pb/^{238}U$ ratios and dates for Palaeozoic zircon. Figure 6 therefore shows a Wetherill concordia plot and the linear regression upper intercept age of 371 ± 6 Ma (MSWD = 0.56, 19 analyses) is interpreted as the time of igneous crystallization.

FO1313 is a metapsammite from Isla Huapi, Lago Ranco, belonging to the Trafun metamorphic complex (the host rock of the monzogranite boulder FO1320). According to Correa (2014) this rock has well-developed $S_1$ and incipient $S_2$ foliations, and is composed of angular clasts (<0.5 mm long) of quartz (40%), K-feldspar (10%), plagioclase (10%), detrital biotite (1%) and muscovite (2%), opaque minerals and rutile (2%), with traces of

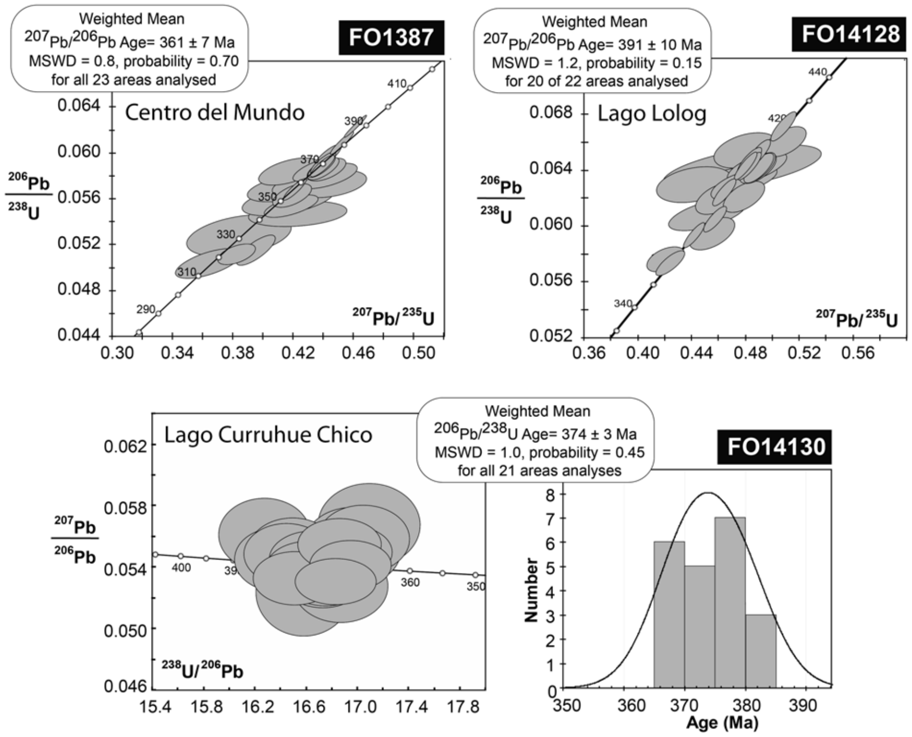


**Fig. 5.** Composite Wetherill plots for samples FO1387 and FO14128. Tera–Wasserburg and age v. probability plots for sample FO14130.

carbonate, tourmaline and zircon, in an argillaceous matrix. The youngest age grouping of six $^{206}Pb/^{238}U$ ages in the probability density plot is within uncertainty of the Tera–Wasserburg concordia, and these ages have a weighted mean of 357 ± 4 Ma (six grains, MSWD = 0.3). Other well-populated peaks occur at *c.* 390 and 469 ± 4 Ma (nine grains, MSWD = 0.9). There are subordinate clusters at *c.* 530 and *c.* 580 Ma (13 grains have ages between 500 and 700 Ma) and 1000–1250 Ma, as well as some Palaeoproterozoic and Archaean zircon grains (Fig. 7).

### *Llanquihue metamorphic complex*

LM1 is a quartz–white mica banded psammopelitic schist with accessory albite, titanite, epidote and zircon. It comes from the base of a 2850 m hydrocarbon exploration borehole near Los Muermos in the Osorno–Llanquihue basin (Fig. 2). Seventy grains were analysed; they show a wide range of ages. Four scattered analyses younger than 350 Ma are significantly enriched in common Pb, are interpreted as having lost radiogenic Pb and so are not reliable crystallization ages. The dominant feature of the age spectrum is the Devonian peak (Fig. 7), which has a weighted mean $^{206}Pb/^{238}U$ age of 385 ± 3 Ma (17 grains, MSWD = 1.4). There is a secondary grouping at 411 ± 4 Ma (five grains, MSWD = 0.7) and minor peaks at 475 Ma and, broadly, 1100 Ma. A very few grains gave Palaeoproterozoic and even Archaean ages.

LM2 is a white mica–chlorite–albite–quartz schist, with clinozoisite, tourmaline, titanite and zircon as accessory minerals. A well-developed $S_1$ main foliation is openly folded by an $S_2$ structure. This rock comes from the bottom of another borehole in the Osorno–Llanquihue basin (1615 m deep). The U–Pb zircon age data are comparable with those for LM1 with a majority of ages in the range 350 – 670 Ma, but in this case with some more prominent components in the age spectrum (Fig. 7). Apart from a single Carboniferous age, discounted on the basis of high

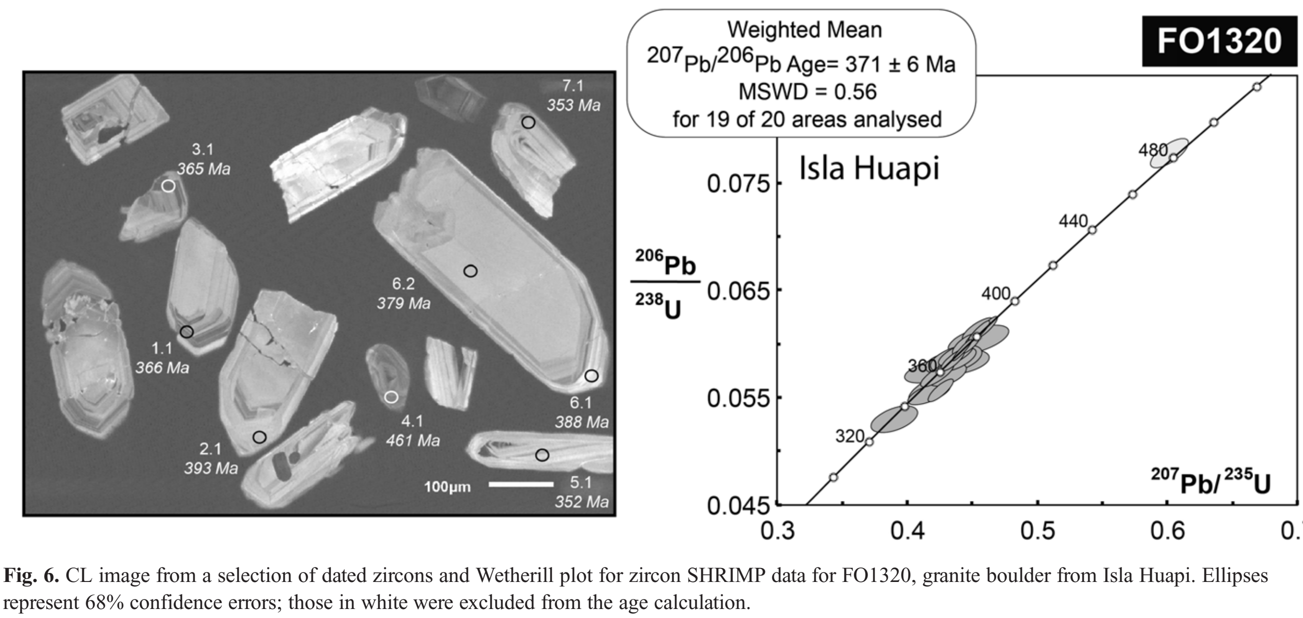


**Fig. 6.** CL image from a selection of dated zircons and Wetherill plot for zircon SHRIMP data for FO1320, granite boulder from Isla Huapi. Ellipses represent 68% confidence errors; those in white were excluded from the age calculation.

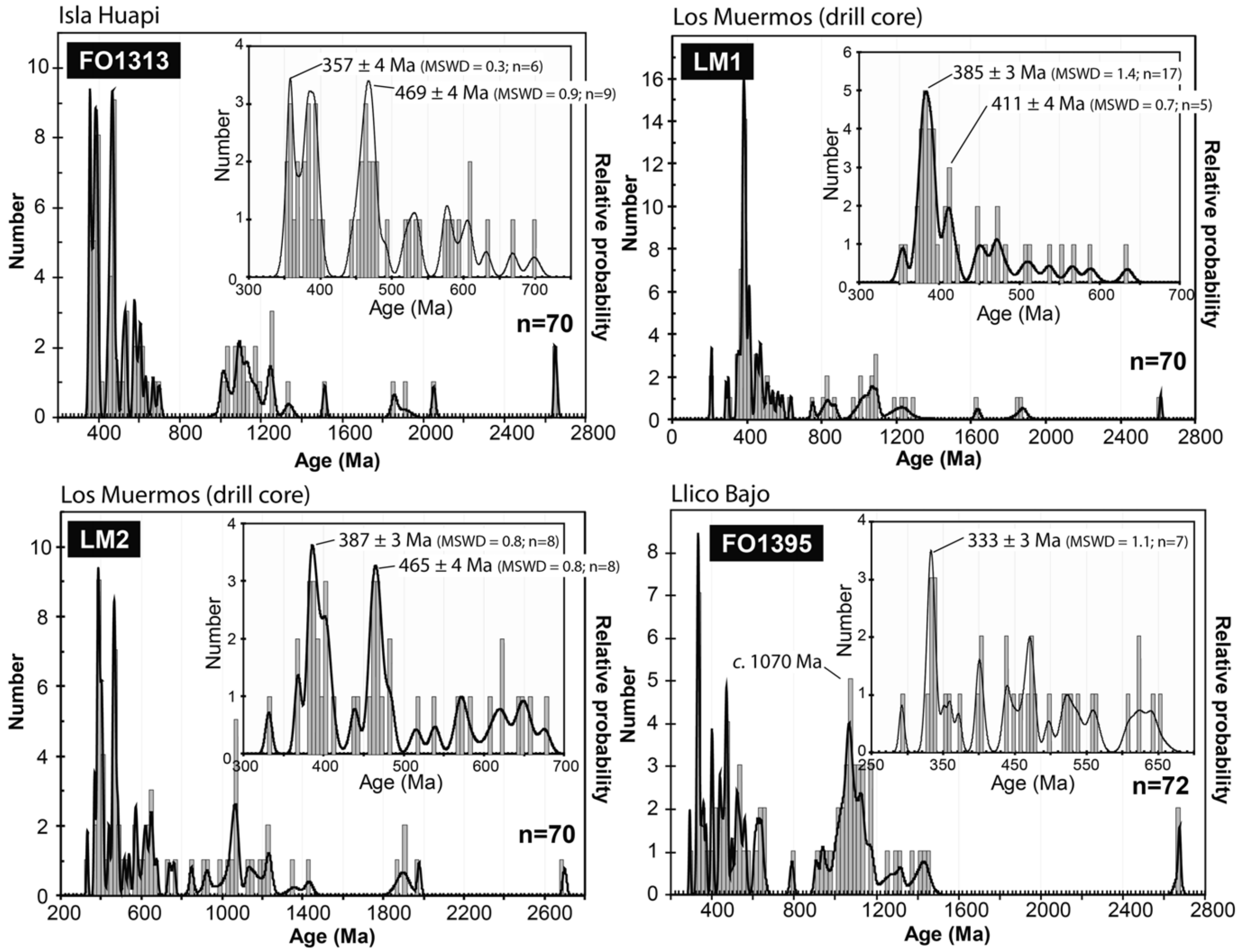


**Fig. 7.** Composite age v. probability diagrams for samples FO1313, LM1, LM2 and FO1395.

common Pb and probable radiogenic Pb loss, the youngest are two analyses with $^{206}Pb/^{238}U$ ages of *c.* 368 Ma, which could be significant. The main Devonian peak at 387 ± 3 Ma (eight grains, MSWD = 0.75) is indistinguishable from that in LM1. There are minor peaks at *c.* 400 and *c.* 440 Ma, and a prominent one at 465 ± 4 Ma. There are other significant but minor peaks in the range 570–670 Ma. There is a well-represented Mesoproterozoic population (mainly 1070 Ma, but possibly also 1240 Ma), with scattered Palaeoproterozoic and one Archaean ages.

### *Bahia Mansa metamorphic complex*

FO1395 is a sample of banded, well-foliated, white mica–quartz schist with albite porphyroblasts from Llico Bajo. Following the nomenclature of Duhart (1999), it belongs to the 'Metamorfitas de Rio Llico' unit within the Bahia Mansa metamorphic complex, near the contact with the 'Metabasitas de Estaquilla'. Pyrite crystals are conspicuous. A wide range of Early Palaeozoic, as well as Neoproterozoic and Mesoproterozoic, zircon grains are present in the rock (Fig. 7). The most prominent (and youngest) peak in the age spectrum has a weighted mean $^{206}Pb/^{238}U$ age of 333 ± 3 Ma (seven grains, MSWD = 1.07), with other notable, but minor groupings at *c.* 400, 440 and 470, and a broad highly populated 'Grenvillian' cluster centred on *c.* 1070 Ma. There are scattered minor dates at *c.* 525, 635, 1130 and 1440 Ma, with two Archaean grains.

FO14101 is a metapsammitic quartz–white mica schist from Playa Guabun, at the northwestern end of Chiloé island. The detrital zircon age distribution is broad, from 320 to 2740 Ma, albeit with a gap from 1200 to 1750 Ma. The best defined peak is also the youngest, at 328 ± 4 Ma (11 grains, MSWD = 0.7), but there is also a major peak at 480 ± 5 Ma (also 11 grains, MSWD = 0.7). There are only a few Devonian or Silurian grains, with three analyses at *c.* 555 Ma and four at *c.* 860 Ma. There is a minor group of 'Grenvillian' ages (*c.* 1110 Ma), a few Palaeoproterozoic ages (*c.* 1940 and *c.* 2250 Ma) and two at 2750 Ma (Fig. 8).

FO14103 is a metasandstone from the Bahia Mansa metamorphic complex near Los Muermos. The three widely scattered, notably young dates associated with high common Pb contents are discounted, as they are thought to be from areas that have lost radiogenic Pb. Apart from sparse Early Palaeozoic and 'Grenvillian' ages, the spectrum is mostly in the range 340–410 Ma (Fig. 8). This dominant clustering has an irregular distribution that can be deconvolved into a major group of 28 grains at 380 ± 4 Ma (MSWD = 0.9), a younger closely spaced sub-group at 366 ± 4 Ma (15 grains, MSWD = 1.0), and possibly an even younger one at 353 ± 4 Ma (six grains, MSWD = 0.7). Further SHRIMP analyses with optimized dating protocols in geochronology mode would be necessary to refine these age groupings, but Devonian provenance is obviously the most important.

### *North Patagonian massif*

FO14122 is a coarse-grained micaschist, present as a large enclave in the Devonian tonalite at San Martin de los Andes in the North Patagonian Massif (Fig. 8). The $^{206}Pb/^{238}U$ ages obtained from detrital zircon are widely scattered: more than half fall in the range 390 Ma (two ages) to 650 Ma, with the main resolvable peaks at 420 ± 5 Ma

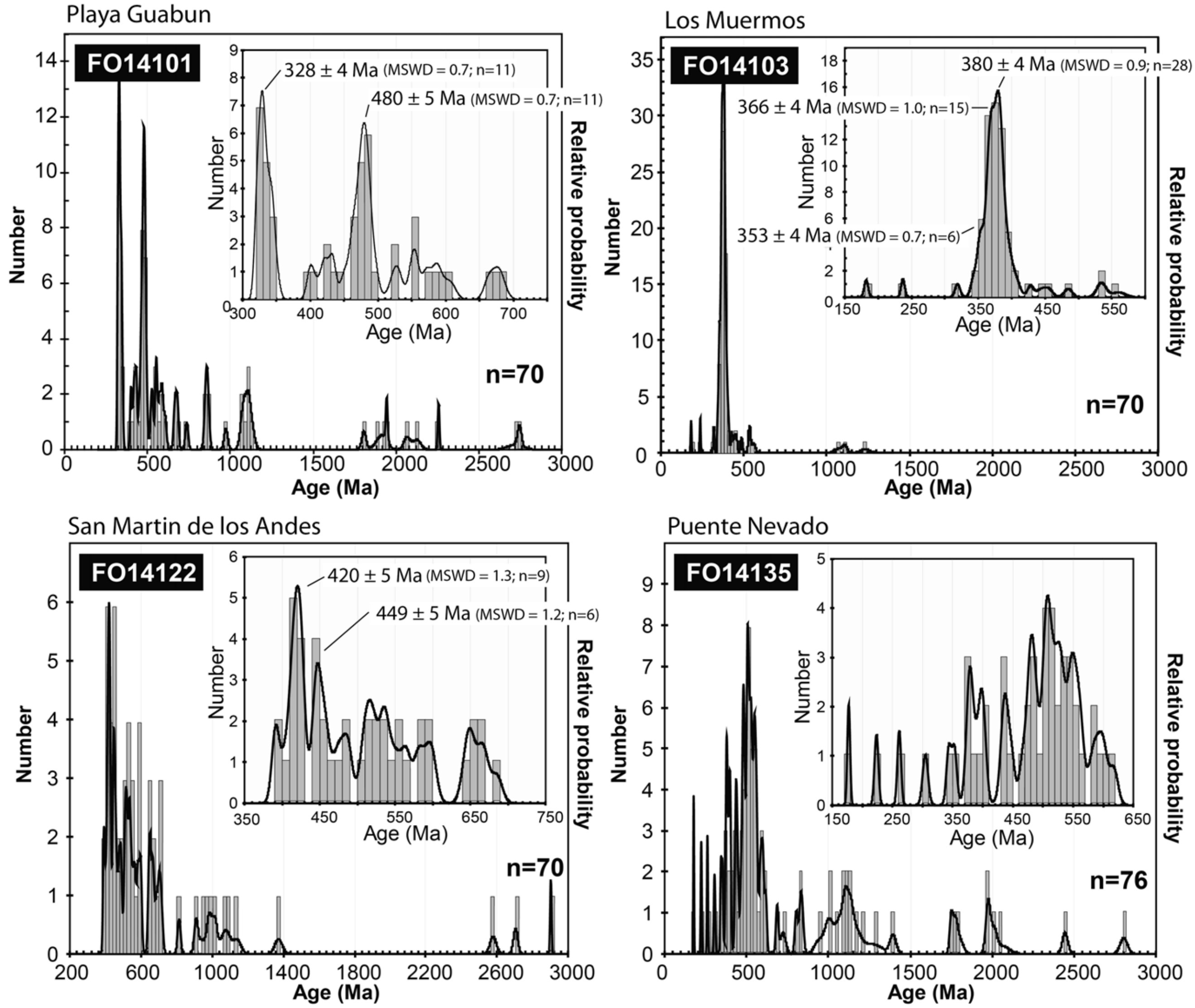


**Fig. 8.** Composite age v. probability diagrams for samples FO14101, FO14103, FO14122 and FO14135.

(nine grains, MSWD = 1.3) and 449 ± 5 Ma (six grains, MSWD = 1.2), and lesser ones at *c.* 485, 500–570, *c.* 600 and *c.* 650 Ma. Older ages are difficult to assess owing to a series of discordant analyses and radiogenic-Pb loss implied from the Wetherill concordia plot (not shown here), but the most concordant analyses have groupings at 900–1100 and, less certainly, 2500–2900 Ma.

FO14135 is a sample of biotite–muscovite gneiss from Puente Nevado near Paso Carirriñe, an international pass across the Andes. This rock was included in the unit known as Liquiñe Gneiss by Hervé (1977), who suggested correlation with the Colohuincul Formation in Argentina. The zircon age spectrum is complex with a wide range (Fig. 8). Four analyses of thin rim areas yield scattered Mesozoic dates, which are anomalous and probably reflect new metamorphic growth during gneiss formation. The bulk of the ages fall between 350 Ma (two ages) and 600 Ma, with apparent peaks at *c.* 380, 400, 440, 485, 510, (525), 550 and 600 Ma. It is noteworthy that the distribution has prominent sub-groupings at about 485, 510 and 550 Ma, which is unusual in comparison with other samples in this study. The older components are again subject to mild discordance, but ages of 835, 1010, 1110, 1750 and 1980 Ma may be significant.

### *Rocks with ages younger than Palaeozoic*

This section summarizes data from rocks considered as possibly Devonian when they were sampled, but that yielded younger U–Pb zircon ages, wholly or in part (Table 2). The results are reported here for elucidation and future reference.

#### *Coast Range*

FO1397 is a foliated and banded metadiorite, previously mapped as belonging to the Bahia Mansa metamorphic complex at Llico Bajo (as was the following sample, FO1399). It consists of coarsely crystalline bands, 20–30 cm wide, alternating with thinner quartz-rich bands. Coarse hornblende and saussuritized plagioclase porphyroclasts are seen in a foliated matrix composed of epidote, chlorite, actinolite and quartz. Dating of a limited number of the complexly structured, heterogeneous zircon population from this rock yielded a predominant grouping of Cretaceous ages (seven out of 12 in the range 129–153 Ma, with a possible peak at *c.* 137 Ma). There are two grains at *c.* 200 Ma and single grains at 455 and 855 Ma (Fig. 9). The intrusion is probably Cretaceous in age.

FO1399 is a massive to faintly schistose green rock, with elongated quartz-rich, ellipsoidal vein-like bodies parallel to the foliation, spaced at 20–30 cm. The mineralogy is amphibole, epidote, and lesser amounts of plagioclase, quartz and titanite. A remarkably simple population of prismatic, euhedral igneous zircons all record earliest Paleocene $^{206}Pb/^{238}U$ ages with a weighted mean of 65.0 ± 0.6 Ma (18 analyses, MSWD = 1.7), which is interpreted as an igneous crystallization age (Fig. 9).

**Table 2.** *U–Pb zircon SHRIMP data for samples with post-Palaeozoic ages*

| Sample number | Location | Geographical coordinates | Lithology | Age (Ma) | Observations |
|---|---|---|---|---|---|
| FO1397 | Llico Bajo beach | 41°17.467′S, 73°50.627′W | Foliated and banded metadiorite | 137 ($n = 12$) | Single population |
| FO1399 | South of Llico Bajo beach | 41°19.335′S, 73°50.026′W | Schistose amphibolite | 65.0 ± 0.6 ($n = 18$) | Single population |
| FO1378 | Termas del Amarillo | 42°59.585′S, 72°26.223′W | Biotite tonalite vein | 9.2 ± 0.1 ($n = 23$) | Single population |
| FO1379 | Termas del Amarillo | 42°59.585′S, 72°26.223′W | Plagioclase–biotite gneiss | 9–1964 ($n = 37$) | |
| FO1383 | Puente Caballo Muerto | 43°08.584′S, 72°26.434′W | Muscovite gneiss | 137 ± 1 (12 rims) | Cores 400 – 2700 Ma, mainly 600 – 700 Ma |
| FO1384 | Puente Caballo Muerto | 43°08.584′S, 72°26.434′W | Muscovite–tourmaline pegmatite | 143 ± 1 ($n = 13$) | |
| FO14109 | Punta Peters | 39°39.400′S, 72°16.792′W | Arkose | 223 ± 3, 284 ± 2 ($n = 71$) | 1 Devonian; 2 late Carboniferous grains |
| FO1389 | Rio Palena bridge | 43°18.524′S, 71°59.551′W | Tuffaceous sandstone | 133.2 ± 0.9 ($n = 13$) | 1 Devonian; 2 late Carboniferous grains |

### *Main Andean range*

FO1378 is a biotite tonalite dyke, <1 m wide, cross-cutting foliated quartz–plagioclase–biotite gneiss (FO1379, see below) at Termas de Amarillo (Fig. 2). Zircons from the tonalite show both oscillatory and sector zonation under CL imaging, and have an exceptionally wide range in U from low to moderate values around 100–500 ppm to extreme values up to at least 10 700 ppm. All 24 area analyses record Miocene $^{206}Pb/^{238}U$ ages but with a very irregular distribution on a probability density plot. At such a young age, it is not possible to calculate radiogenic $^{207}Pb/^{206}Pb$ ages and so an estimate for the magmatic crystallization age can be obtained for a weighted mean of the more dominant, and lower U, $^{206}Pb/^{238}U$ ages of 9.2 ± 0.1 Ma (23 analyses, MSWD = 1.8; Fig. 10)

The gneiss FO1379 has centimetre-scale bands of granitic composition parallel to the foliation. It has a complex and heterogeneous population of zircon grains that record an extended and diffuse age spectrum, ranging from *c.* 9 to *c.* 1964 Ma) with no clear predominant groupings (Fig. 10). Analyses of rim areas with CL characteristics interpreted as metamorphic have Th/U ratios <0.01 and $^{206}Pb/^{238}U$ ages younger than 180 Ma, whereas the inherited central parts of grains are older than 315 Ma and have Th/U ratios higher than 0.02. This indicates that Mesozoic and younger zircon formed as metamorphic rims on existing older components, and so the maximum possible sedimentation age cannot easily be estimated.

FO1383 from Puente Caballo Muerto (Fig. 2) is a well-foliated banded muscovite-bearing augen gneiss, cut by foliated mafic dykes. The gneiss has a quartz–plagioclase–muscovite–biotite–garnet assemblage, and centimetre-wide leucocratic bands of granitic composition folded by shear zones with horizontal lineation. It can be considered a metatexite, and has a heterogeneous population of zircon grains. The zircon age pattern is complex (Fig. 10). Analyses of the central components of the grains have Th/U values greater than 0.11 (mostly >0.2) and ages ranging from 400 to 2760 Ma, among which a group of six at 590–660 Ma is conspicuous. In contrast, analyses of 25 rim components with low Th/U ratios (≤0.11) record Cretaceous $^{206}Pb/^{238}U$ ages ranging from 131 to 149 Ma, of which 14 have a weighted mean of 137 ± 1 Ma (MSWD = 0.7). Some of the rim areas analysed are in the same grains as the older inherited cores and so this Cretaceous age is interpreted as the time of metamorphism. Apparent older ages obtained from some low Th/U values are considered to reflect mixed U–Pb systematics.

The gneiss FO1383 is intruded by a muscovite–tourmaline pegmatitic vein FO1384, which also has a complex and heterogeneous zircon population and an age distribution showing the same general features. The few dated cores, with Th/U > 0.3, gave scattered Palaeozoic and Mesoproterozoic ages up to 1500 Ma, whereas zircon rims with high U contents and Th/U < 0.01 are Mesozoic (131–163 Ma). A weighted mean for 13 rim analyses gave a Cretaceous $^{206}Pb/^{238}U$ age of 143 ± 1 Ma with a high MSWD value of 2.1 (Fig. 10), which is taken as recording crystallization of the low-temperature igneous pegmatite.

FO14109 is a meta-arkose from Punta Peters, on the shore of Lago Panguipulli. The arkose is interstratified with quartz conglomerates; this is typical of the Triassic Panguipulli Formation, which Campos *et al.* (1998) differentiated from the Trafun metamorphic complex (with which it was combined in some previous maps). Apart from four ‘Grenville-age’ zircon grains, the age spectrum comprises a more prominent Permian cluster and a smaller Triassic grouping. The Permian analyses form a bimodal distribution that can be resolved into two sub-groups, 30 grains with a prominent peak at a weighted mean $^{206}Pb/^{238}U$ age of 284 ± 2 Ma (MSWD = 0.8) and the remaining 20 with a mean of 297 ± 3 Ma (MSWD = 0.8, Fig. 11). Eight Triassic detrital zircons provide a maximum possible sedimentation age of 223 ± 3 Ma (MSWD = 0.5) and support correlation of these rocks with the Panguipulli Formation.

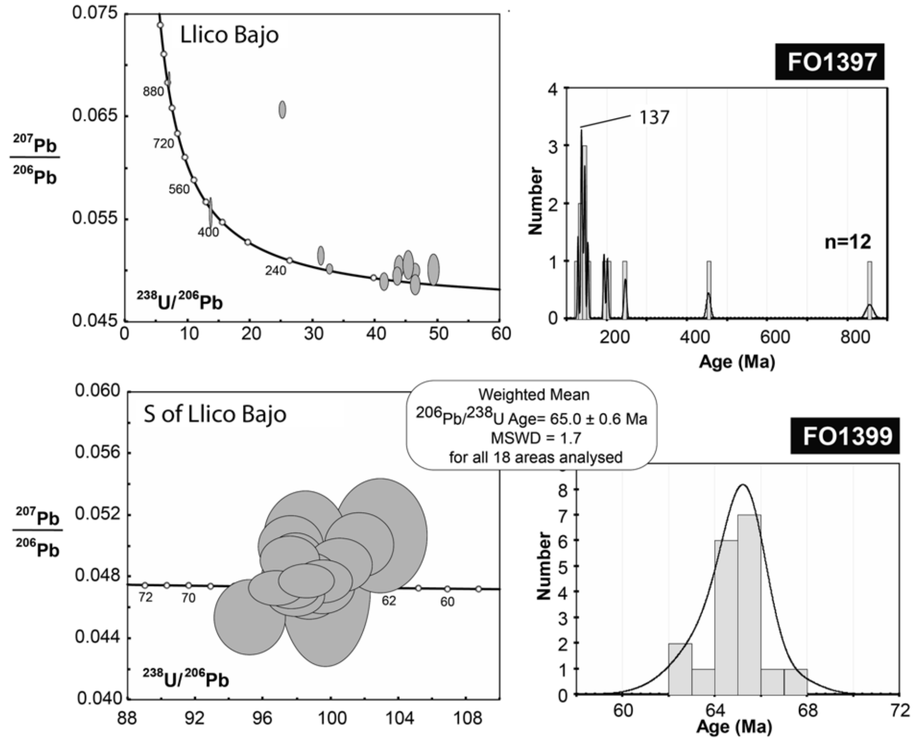


**Fig. 9.** Tera–Wasserburg and age v. probability diagrams for samples FO1397 and FO1399.

FO1389 from Puente Río Palena is an epiclastic sandstone with calcareous cement and fossil plants, which has a remarkable zircon population dominated by oscillatory-zoned igneous grains. Thirteen of these indicate an Early Cretaceous maximum possible sedimentation age with a weighted mean $^{206}Pb/^{238}U$ age of 133 ± 1 Ma (MSWD = 0.6, Fig. 11). Four older zircon grains (one Jurassic, two Early Permian and one Devonian) were also analysed, as well as one totally anomalous grain dated at 90 Ma (possibly a contaminant). These ages suggest that the majority of zircon grains in this sample were derived from a contemporaneous magmatic source, and that few other lithologies were shedding detritus to this part of the Palena basin during deposition.

## Zircon Lu–Hf and O isotopes

The results of Hf- and O-isotope analyses are plotted in Figure 12. The main focus of the Lu–Hf and O-isotope analyses has been the zoned igneous zircon in Devonian intrusive bodies, and Devonian zoned igneous detrital zircons in metasedimentary rocks from a range of the units. Also plotted in Figure 12 are a number of zoned igneous detrital zircons with mainly Ordovician and Permian ages.

The initial Hf-isotope compositions are expressed in epsilon units calculated at the zircon crystallization age ($\varepsilon Hf_t$). For the Devonian intrusive bodies in Chile (Pichicolo and Chaitén) values range from +5 to +13, indicating a significant radiogenic component ascribed to depleted mantle in the source of these magmatic zircon grains. In contrast, Devonian igneous rocks on the eastern side of the Andes in Argentina have markedly lower $\varepsilon Hf_t$, varying from −5 to +5. This indicates the presence of more unradiogenic Hf in the magma source (s) of the Argentine Devonian igneous zircon.

Devonian detrital igneous zircon grains in the Chilean accretionary complex metasedimentary rocks have $\varepsilon Hf_t$ values between +7 and −6, markedly lower than those for corresponding igneous rocks in Chile. The Ordovician, Carboniferous and Permian detrital igneous zircons have similar $\varepsilon Hf_t$ values, but with a more limited range from +2 to −5.

On a $\delta^{18}O$ v. age plot it can be seen that the zircons from the two Devonian intrusive rocks in the accretionary complex from the present western slope of the Andes have $\delta^{18}O$ values between +5.2 and +3.7‰. These values overlap with, but on average tend to be lower than, those for zircon with mantle $\delta^{18}O$ (+5.3 ± 0.6‰; Valley *et al.* 1998), indicating that the source of the magmas from which these zircons crystallized has not interacted with crustal rocks. In contrast, zircons from the three intrusive bodies in the eastern slope of the Andes have significantly higher positive $\delta^{18}O$ values (+5.6 to +6.4‰ for the Lago Curruhue Chico granite, +6.4 to +8.6‰ for the Lago Lolog granite, and +6.7 to +8.2‰ for the San Martin de los Andes tonalitic gneiss). These Argentine igneous zircons have crystallized from magmas that have generally incorporated crustal (sedimentary) sources.

Most of the Devonian detrital zircons present in the metasedimentary rocks of the accretionary complexes in coastal Chile have $\delta^{18}O$ values similar to those in the contemporaneous plutonic bodies in Argentina, and only a few grains have low $\delta^{18}O$ values comparable with those of the intrusive rocks in Chile. This indicates that the source of the Devonian igneous detrital zircons was not the local Chilean Devonian magmatic rocks with mantle-like zircon $\delta^{18}O$ values. The detrital igneous zircons with Ordovician ages have somewhat higher values (6.8–10.1‰, average +8.5‰) than those of Devonian (4.2–10.1‰, average +7.5‰) and Carboniferous–Permian (4.4–8.4‰, average +6.9‰) age. There is no consistent distinction in the composition of detrital zircons between Western and Eastern Series of the accretionary complex, either in $\varepsilon Hf_t$ or $\delta^{18}O$ values.

## Discussion

### *Igneous geochronology*

There is now considerable evidence for Devonian magmatism in this region. The ages of three igneous rocks in Chile previously dated as Devonian (Campos *et al.* 1998; Duhart *et al.* 2001; Duhart 2008) have been confirmed and refined in this study: the Pichicolo tonalite (384 ± 3 Ma), the Chaitén metatonalite (383 ± 2 Ma), and a granitic clast in conglomerate at Isla Huapi (371 ± 6 Ma). Granite at Lago Lolog in Argentina gave a preferred $^{207}Pb/^{206}Pb$ age of 391 ± 10 Ma, compatible with a previous result of 395 ± 4 Ma (Pankhurst *et al.* 2006), and a new Devonian igneous crystallization age was

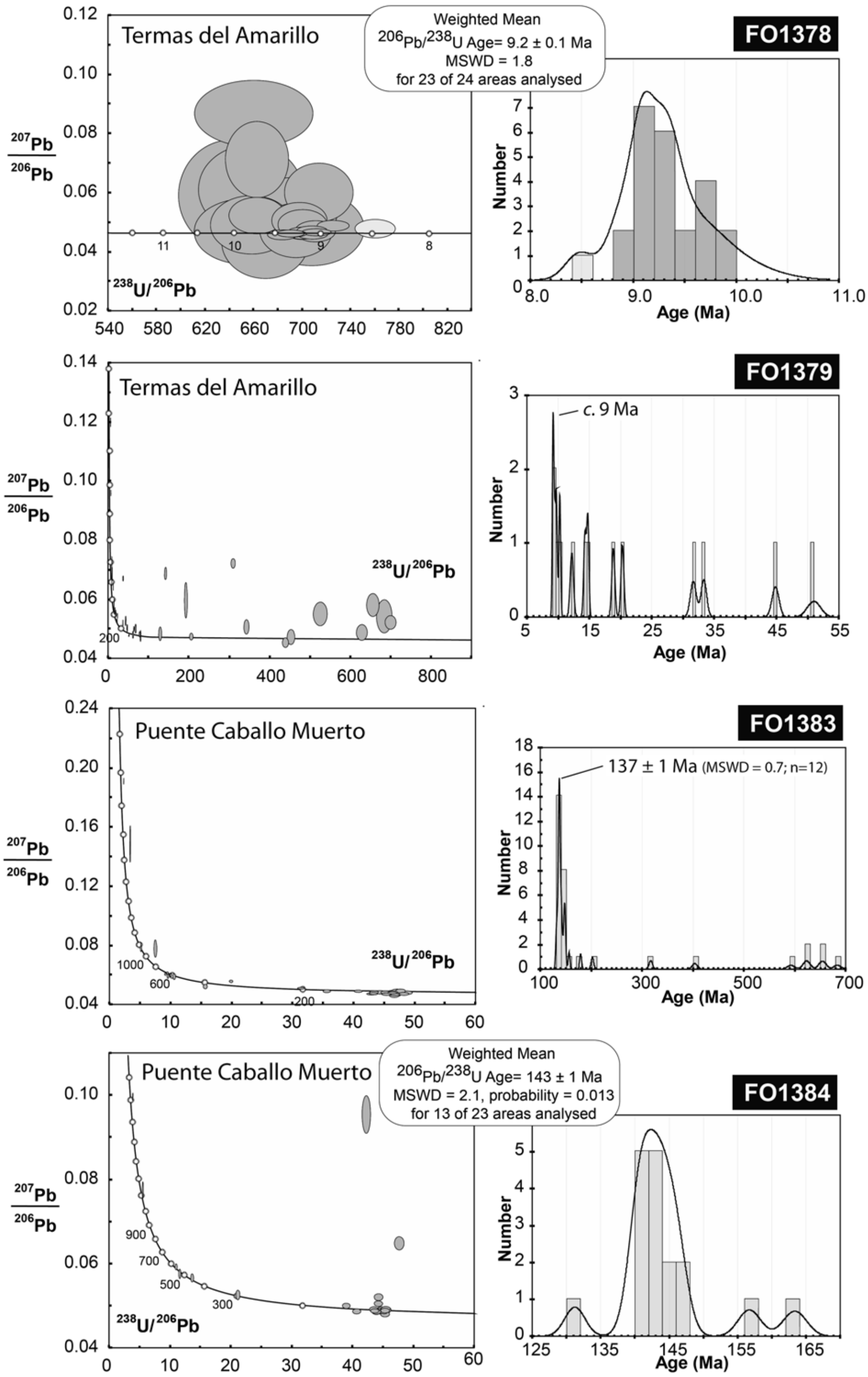


**Fig. 10.** Tera–Wasserburg and age v. probability diagram for samples FO1378, FO1379, FO1383 and FO1384.

obtained for granodiorite at Lago Curruhue Chico (374 ± 3 Ma). The partially deformed tonalite body at San Martín de los Andes has given somewhat older dates of 394 ± 3 Ma (Godoy *et al.* 2008; Hervé *et al.* 2013) and 401 ± 3 Ma (Pankhurst *et al.* 2006), suggesting a 'best' age estimate of 397 ± 4 Ma. However, Pankhurst *et al*. dated the Gastre granite at 371 ± 2 Ma and the Colán Conhue granite, some 300 km to the SSE, at 394 ± 4 Ma. The Zarao trachyte in the Coast Range (Duhart *et al.* 2001) also appears to be older at 397 ± 1 Ma (based on TIMS analysis of five zircon grains).

The U–Pb SHRIMP zircon data for two gneisses (FO1382 and FO1387) from the Main Range metamorphic complex in the western foothills of the Andes indicate that they are orthogneisses, and that their igneous protolith originally crystallized in the Devonian; it was later deformed and metamorphosed, with Cretaceous growth of zircon rims. Their ages are 364 ± 2 and 361 ± 7 Ma (i.e. latest Devonian). Jurassic, Cretaceous and Miocene plutonic rocks in spatial association with these rocks have been dated here (see below) and elsewhere.

A metasedimentary enclave in the San Martín tonalite has youngest zircons of 420 Ma (or possibly *c.* 390 Ma). A paragneiss in the main range at Puente Nevado near Liquiñe has a younger maximum age of *c.* 380 Ma, which casts doubt on its correlation with the Colohuincul Formation, the country rock of the Devonian intrusions in the North Patagonian Massif.

### *Isotope geochemistry*

The Hf- and O-isotope data indicate very clearly that the Devonian intrusive rocks in the accretionary complex of Chile have a different magma genesis from that of the coeval intrusions into the

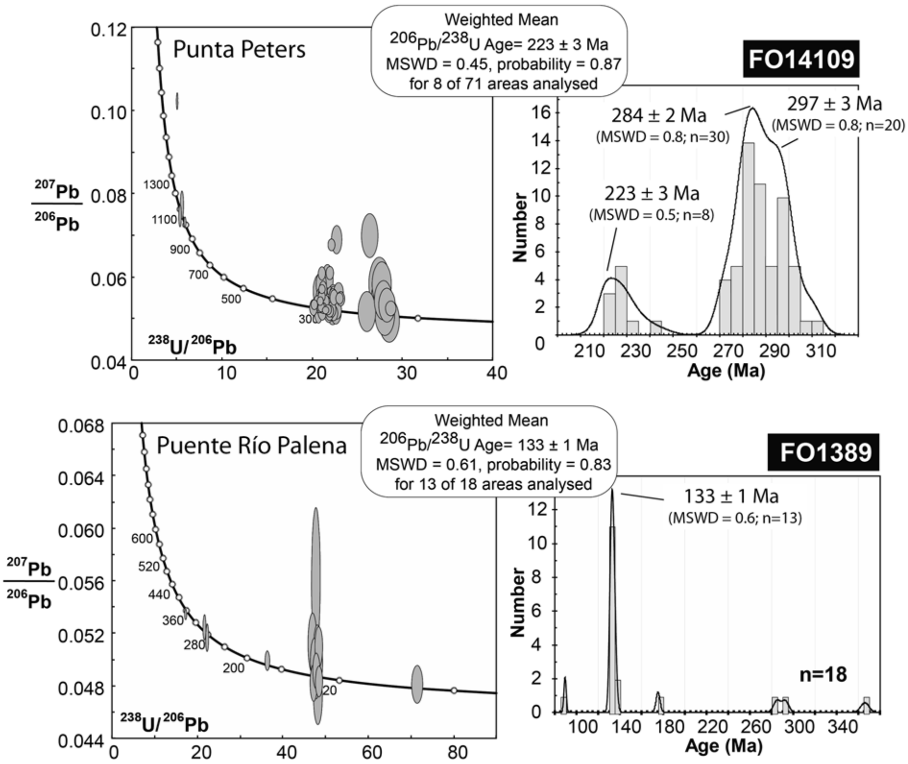


**Fig. 11.** Tera–Wasserburg and age v. probability diagram of samples FO14109 and FO1389.

Colohuincul Formation of the North Patagonian Massif and easternmost Chile in these latitudes (40 – 43°S). The Chilean intrusive rocks have zircons with mantle $\delta^{18}$O isotope compositions and primitive $\varepsilon Hf_t$ values, whereas those from Argentina are derived from magmas that were more enriched in crustal components. The country rocks of the Devonian intrusions in Chile are characterized by the presence of abundant mafic and some ultramafic rocks, together with continent-derived metasedimentary rocks, in marked contrast to the mainly argillaceous character of the Colohuincul Formation of the North Patagonian Massif. The Devonian detrital igneous zircons in the Chilean accretionary prism have $\delta^{18}$O and initial Hf ratios that are clearly related to the Argentine igneous sources, with very few derived from the more mantle-like Chilean intrusive sources.

The Devonian tonalites at Pichicolo and Chaitén have a suprasubduction-zone calc-alkaline geochemistry (Quezada 2015). Similarly, metabasites associated with the Chaitén tonalite, as well as the metabasite clast in the conglomerate from the Trafun Formation at Isla Huapi, have arc-related geochemistry. In contrast, the Zarao 'trachyte' (or rhyolite, Quezada 2015), has geochemical affinities with mid-ocean ridge or oceanic island siliceous igneous

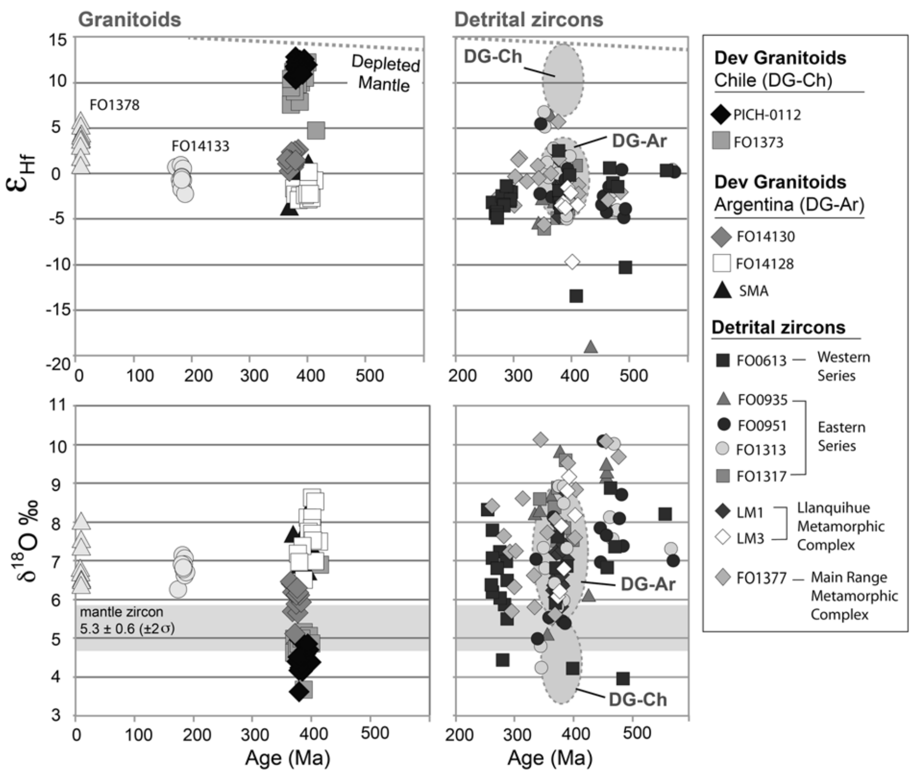


**Fig. 12.** Hf- and O-isotope data for Devonian igneous rocks and orthogneisses (left-hand column), and for (mostly) Devonian detrital zircon grains in the analysed metamorphic rocks (right-hand column). In the latter, DG-Ch and DG-Ar are the respective fields for the Devonian igneous rocks of the western outcrops in Chile and the eastern outcrops, mostly in Argentina. The dotted lines in the Hf plots represent the depleted mantle trend.

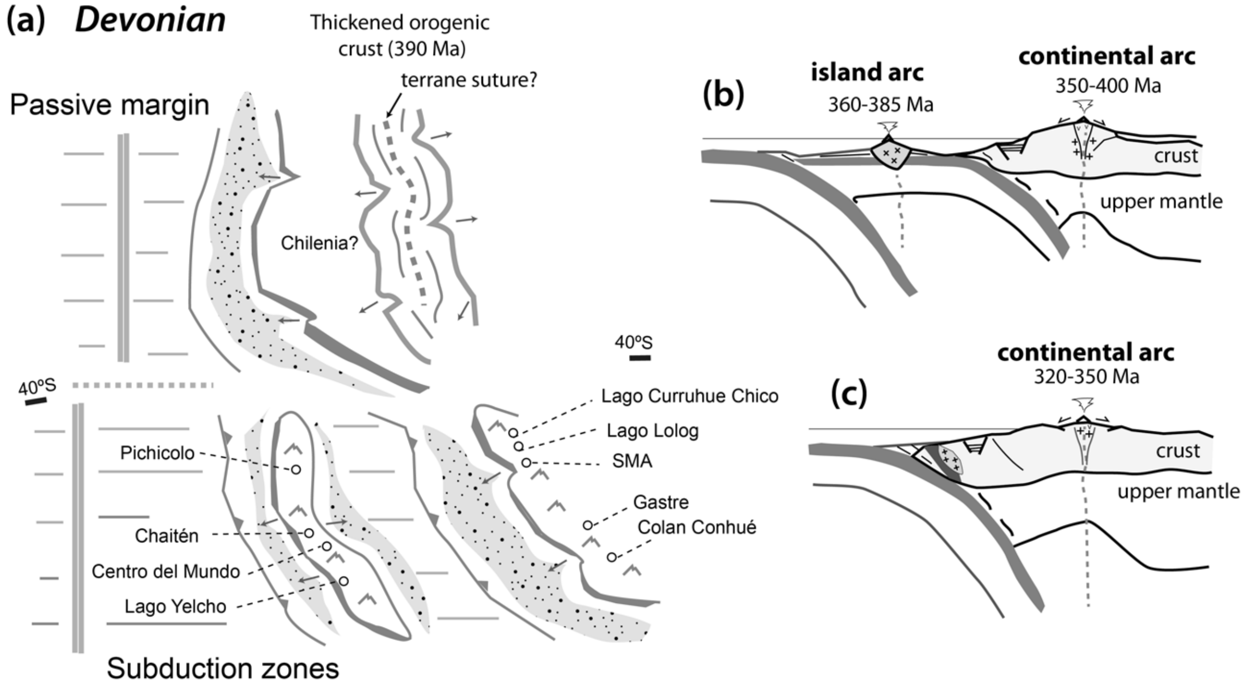


**Fig. 13.** (**a**) Palaeotectonic sketch map (after Hervé *et al.* 2013), showing the Devonian double subduction zone model proposed in this paper. (**b**) shows an oceanic island-arc represented by the western belt of juvenile granitoids emplaced in the accretionary complex and an essentially synchronous continental arc represented by the eastern Andean granitoids. After collision and partial delamination (**c**), probably in late Devonian times, a single subduction zone continued to produce the juvenile Early Carboniferous magmas on the western border of the North Patagonian Massif (Pankhurst *et al.* 2006).

rocks, and in this case spatially associated metabasites have MORB-like geochemistry (Díaz *et al.* 1988; Duhart 1999).

### *Detrital zircon provenance*

The age of the Zarao trachyte, 397 Ma (Duhart *et al.* 2001), is not in accord with our detrital zircon age constraints on the Bahia Mansa metamorphic complex, which is younger: the maximum possible sedimentation age for the micaschist at Llico Bajo (FO1395) is 333 ± 3 Ma. Essentially the same maximum possible depositional age (328 ± 4 Ma) was determined for schists at Playa Guabun, in the NW corner of Chiloé island, in essentially the Lacui metapelites unit of Duhart (1999). Metasandstones of the Western (FO14103) and Eastern Series (FO1313) have maximum depositional ages of *c.* 355 Ma respectively.

However, in two micaschists from the boreholes in the Osorno–Llanquihue basin, the youngest significant detrital zircon ages are 385 ± 3 Ma (LM1) and 387 ± 4 Ma (LM2), respectively, which are much closer to the igneous crystallization age of the Zarao trachyte, albeit still somewhat younger. The age of the metabasites into which the Zarao trachyte was emplaced is not known, and it is conceivable that the trachyte was contemporaneous with the basic rocks, in a mid-ocean ridge or oceanic island environment, prior to sedimentation of the protolith of the micaschists and their amalgamation into the accretionary prism, as this portion of the ocean floor approached the subduction zone.

The significantly older maximum possible sedimentation age determined for the borehole schist samples, compared with those of the Bahia Mansa metamorphic complex, is in agreement with the interpretation of M. R. McDonough *et al*. (pers. comm.) that a different, older basement is found at these depths. McDonough *et al.* referred to this as the Llanquihue basement complex, and presented metamorphic cooling ages of 359–386 Ma on various rock types; that is, older than the metamorphic ages (292–319 Ma) of the Western Series at Pichilemu (34°S; Willner *et al.* 2005). The Early Devonian ages from this part of the accretionary complex were interpreted by Kato (1985), Kato & Godoy (1995) and Kato *et al.* (2008) as corresponding to an early metamorphic event in the subduction-zone margin of Gondwana. The age span of these early events corresponds broadly to the ages of the intrusive rocks in the western slope of the Andes (*c.* 385 and *c.* 380 Ma) and of the somewhat younger Main Range orthogneisses presented here (*c.* 365 and *c.* 360 Ma), as well as to those in the western margin of the North Patagonian Massif (*c.* 375 and *c.* 400 Ma), all of which are very probably related to the initial subduction in this segment of the Gondwana continental margin. The oldest maximum possible sedimentation ages are indicated by schists intruded by the plutonic rocks at San Martin de los Andes, whose youngest zircons are Silurian (420 Ma).

The Hf- and O-isotope data and ages obtained in this study favour provenance of the Isla Huapi conglomerate clasts from Devonian magmatic rocks similar to those located east (present coordinates) of the outcrop. This further suggests that at these latitudes the Trafun metamorphic complex was deposited in a fore-arc basin and not on the passive-margin platform that is thought to be the depositional environment of the Eastern Series to the north of 38°S.

### *Mesozoic and Cenozoic imprint*

Our evidence also shows that the Devonian magmatic rocks emplaced along what is now the western flank of the modern Andes were intruded into the Main Range metamorphic complex (Hervé *et al.* 2003) and were subject to deformation and high-*T* metamorphism during Early Cretaceous times, namely between *c.* 145 and *c.* 135 Ma. Much later, Late Miocene magmatism is exemplified by the *c.* 9 Ma granite dyke intrusion. These processes led to the growth of rims on the detrital zircon crystals in the surrounding gneisses, thus partly obscuring the original detrital zircon age patterns for these rocks. Deposition of volcaniclastic rocks at the Palena bridge, was constrained at *c.* 135 Ma for a sample with practically no other detrital zircon component, testifying to magmatic activity in the Early Cretaceous.

Cretaceous to Miocene plutonic activity has been established for the North Patagonian batholith (Munizaga *et al.* 1988; Pankhurst *et al.* 1999; Duhart *et al.* 2006) and intense Cenozoic crustal deformation then occurred along the Liquiñe–Ofqui Fault Zone (Cembrano *et al.* 1996). These processes appear to have strongly affected the Devonian plutonic rocks, obscuring their recognition and amenability to dating.

More surprising has been the dating of foliated green rocks of Early Cretaceous age (*c.* 145 Ma) and of Early Cenozoic age (65 Ma) in the coastal outcrops of the Metabasitas de Estaquilla unit of the Bahía Mansa metamorphic complex of Duhart (1999). These rocks seem to be foliated and metamorphosed diorites and they testify to previously unknown Cretaceous and Cenozoic deformational episodes in the Bahia Mansa metamorphic complex, which will not be addressed here.

### *Geotectonic setting*

A simple schematic model to explain these relationships is shown in Figure 13. It is suggested that the western Devonian intrusions represent an oceanic island arc formed above an easterly dipping subduction zone located to the west of the continental subduction margin. The island-arc subduction magmatism was essentially coeval with (or slightly younger than) the continental magmatic belt on the eastern side of the present Andes. After collision and accretion of the island arc, probably long before 300 Ma, the subduction activity continued with the formation (in a slightly different location) of a juvenile Early Carboniferous arc (Pankhurst *et al.* 2006). This model differs from the one presented by Chernicoff *et al.* (2013) in that the western magmatic arc is oceanic, and not built over an old continental fragment. This scenario is apparently unconnected with the Ediacaran to Ordovician evolution of the continental crust in the eastern part of the North Patagonian Massif (Rapalini *et al.* 2013; Pankhurst *et al.* 2014).

## Conclusions

In the studied Andean segment (39–42°S) Devonian (353–404 Ma) subduction-related magmatic activity is recorded, in contrast to the passive margin scenario in northern and central Chile. O- and Hf-isotope data distinguish two belts of intrusions: a mantle-derived one in the western slope of the Andes, and one involving continental crust in the North Patagonian Massif, east of the present Andes at these latitudes. Orthogneisses in the western belt show that Cretaceous igneous and metamorphic events affected the Devonian intrusive rocks, obscuring their recognition and amenability to dating. The Devonian detrital zircons of the accretionary complex of the Coastal Range in Chile mostly have a provenance from the North Patagonian belt, as indicated by their O and Hf isotopes, and not from the mantle-derived magmatic belt. A double subduction zone is inferred to have existed in the southwestern margin of Gondwana (Fig. 13). There is no significant continental terrane accretion in this Andean segment, as is supposedly the case with the hypothetical Chilenia terrane north of 38°S. Igneous, deformational and metamorphic activity in the accretionary complex in Cretaceous and Early Paleocene times is documented for the first time.

## Acknowledgements and Funding

Project Fondecyt 1130227 financed the research. J. Vargas, Universidad de Chile, separated the zircons. L. Rojas, S. Elegueta and J. Arriagada from Empresa Nacional del Petróleo (ENAP) are thanked for access to cores from hydrocarbon exploration boreholes in the Osorno–Llanquihue basin. P. Duhart, SERNAGEOMIN, participated in the formulation of this project and generously provided unpublished information. I. Dalziel was a stimulating companion in an early field trip. Two anonymous reviewers and the editorial board helped to greatly improve the original text.

*Scientific editing by Martin Whitehouse*

## References

Aguirre, L., Hervé, F. & Godoy, E. 1972. Distribution of metamorphic facies in Chile, an outline. *Kristalinikum*, **9**, 7–19.

Bahlburg, H. & Hervé, F. 1997. Geodynamic evolution and tectonostratigraphic terranes of Northwestern Argentina and Northern Chile. *Geological Society of America Bulletin*, **109**, 869–884.

Campos, A., Moreno, H., Muñoz, J., Antinao, J., Clayton, J. & Martin, M. 1998. *Area de Futrono–Lago Ranco, Mapas Geológicos No. 8, scale 1:100,000.* Servicio Nacional de Geología y Minería, Santiago.

Cembrano, J., Hervé, F. & Lavenu, A. 1996. The Liquiñe–Ofqui fault zone: a long lived intra arc fault system in Southern Chile. *Tectonophysics*, **259**, 55–66.

Chernicoff, C., Zappettini, O., Santos, J., McNaughton, N. & Belousova, E. 2013. Combined U–Pb SHRIMP and Hf isotope study of the Late Paleozoic Yaminué Complex, Rio Negro Province, Argentina: implications for the origin and evolution of the Patagonia composite terrane. *Geoscience Frontiers*, **4**, 37–56.

Correa, J. 2014. *Petrología y proveniencia del Complejo Metamórfico Trafun Devónico–Carbonifero, Lago Ranco, Región de los Rios, Chile*. Graduation thesis, Universidad de Chile, Santiago.

Crignola, P., Duhart, P., McDonough, M. & Muñoz, J. 1997. Antecedentes geoquímicos acerca del origen de los esquistos máficos y cuerpos ultramáficos en la Cordillera de la Costa, sector norte de la Xa Región, Chile. *In*: *8th Congreso Geológico Chileno*, *Antofagasta, Actas II*, 1254–1258.

Cruz Martínez, J., Dristas, J.A. & Massone, H.-J. 2011. Palaeozoic accretion of the microcontinent Chilenia, North Patagonian Andes: high-pressure metamorphism and subsequent thermal relaxation. *International Geology Review*, **54**, 472–490.

Deckart, K., Hervé, F., Fanning, C.M., Ramírez, V., Calderón, M. & Godoy, E. 2014. U–Pb geochronology and Hf–O isotopes of zircons from the Pennsylvanian Coastal Batholith, South–Central Chile. *Andean Geology*, **41**, 49–82.

Díaz, L., Vivallo, W., Alfaro, G. & Cisternas, M.E. 1988. Geoquímica de los esquistos Paleozoicos de Bahía Mansa, Osorno, Chile. *In*: *5th Congreso Geológico Chileno*, *Santiago, Actas II*, E75–E96.

Duhart, P. 1999. *Geología del basamento metamórfico de la Cordillera de la Costa entre los 41°00’–42°00’L.S., X Region, Chile: consideraciones geocronológicas*. Graduation thesis, Universidad de Concepción, Chile.

Duhart, P., McDonough, M., Muñoz, J., Martin, M. & Villeneuve, M. 2001. El Complejo Metamórfico Bahía Mansa en la Cordillera de la Costa del centro-sur de Chile 39°30’–42°00’ S: geocronología K–Ar, Ar/Ar y U–Pb e implicancias en la evolución del margen sur-occidental de Gondwana. *Revista Geológica de Chile*, **28**, 179–208.

Duhart, P., Haller, M. & Hervé, F. 2002. Diamictitas como parte del protolito de las metamorfitas de la Formación Cushamen en Río Chico, Provincias de Río Negro y Chubut, Argentina. *In*: Cabaleria, N., Cingolani, C.A., Linares, E., López de Luchi, M.G., Ostera, H.A. & Panarello, H.O. (eds) *Actas del XV Congreso Geológico Argentino.* Asociación Geológica Argentina, Buenos Aires, CD-ROM Article No. 194.

Duhart, P., Barra, F., Muñoz, J., Nutman, A., Ruiz, J. & Tassinari, C. 2006. Cretaceous and Miocene molybdenite Re–Os and U–Pb SHRIMP zircon ages for intrusive bodies in the Chilean North-Patagonian Andes. *In*: *V South American Symposium on Isotope Geology*, *Punta del Este*, *Abstracts Vol. 1*, 492–495.

Duhart, P., Cardona, A., Valencia, V., Muñoz, J., Quiroz, D. & Hervé, F. 2009. Evidencias de basamento Devónico, Chile centro-sur 41–44°S. *In*: *XII Congreso Geológico Chileno. Servicio Nacional de Geología y Minería*, Santiago, CD-ROM, S8_009.

Duhart, P.L. 2008. *Processos metalogeneticos em ambientes de arco magmático tipo andino, caso de estudo: mineralizacoes da regiao dos Andes Patagónicos setentrionais do Chile*. PhD Dissertation, São Paulo University.

Fortey, R., Pankhurst, R. J. & Hervé, F. 1992. Devonian trilobites at Buill, Chile, 42°S. *Revista Geológica de Chile*, **19**, 133–144.

Glodny, J., Lohrmann, J., Echtler, H., Gräfe, K., Seifert, W., Collao, S. & Figueroa, O. 2005. Internal dynamics of a paleoaccretionary wedge: insights from combined isotope tectonochronology and sandbox modelling of the South–Central Chilean forearc. *Earth and Planetary Science Letters*, **231**, 23–39.

Glodny, J., Echtler, H., Collao, S., Ardiles, M., Burón, P. & Figueroa, O. 2008. Differential Late Paleozoic active margin evolution in South–Central Chile 37°S–40°S—the Lanalhue fault zone. *Journal of South American Earth Sciences*, **26**, 397–411.

Godoy, E., Hervé, F. & Fanning, C.M. 2008. Edades U–Pb SHRIMP en granitoides de Macizo Norpatagónico: implicancias geotectónicas. *In*: *XVII Congreso Geológico Argentino*, *San Salvador de Jujuy, Actas III*, 1288–1289.

Gonzalez-Bonorino, F. & Aguirre, L. 1970. Metamorphic facies series of the crystalline basement of Chile. *Geologische Rundschau*, **59**, 979–994.

Hervé, F. 1988. Late Paleozoic subduction and accretion in Southern Chile. *Episodes*, **11**, 183–188.

Hervé, F., Fanning, C.M. & Pankhurst, R.J. 2003. Detrital zircon age patterns and provenance in the metamorphic complexes of Southern Chile. *Journal of South American Earth Sciences*, **16**, 107–123.

Hervé, F., Calderón, M., Fanning, C.M., Pankhurst, R.J. & Godoy, E. 2013. Provenance variations in the Late Paleozoic accretionary complex of Central Chile as indicated by detrital zircons. *Gondwana Research*, **23**, 1122–1135.

Hervé, F., Fanning, C.M., Calderón, M. & Mpodozis, C. 2014. Early Permian to Late Triassic batholiths of the Chilean Frontal Cordillera (28°–31°S): SHRIMP U–Pb zircon ages and Lu–Hf and O isotope systematics. *Lithos*, **184–187**, 436–446.

Hervé, M. 1977. *Geología del área al E de Liquiñe, Prov. de Valdivia, IX Región. Memoria.* Departamento de Geología, Universidad de Chile, Santiago.

Kato, T. 1985. Pre-Andean orogenesis in the coast ranges of Central Chile. *Geological Society of America Bulletin*, **96**, 918–924.

Kato, T. & Godoy, E. 1995. Petrogenesis and tectonic significance of Late Paleozoic coarse-crystalline blueschist and amphibolite boulders in the coastal range of Chile. *International Geological Review*, **37**, 992–1006.

Kato, T.T., Godoy, E., McDonough, M., Duhart, P., Martin, M. & Sharp, W. 1997. Un modelo preliminar de deformación transpresional Mesozoica y gran desplazamiento hacia el norte de parte de la Serie Occidental, complejo acrecionario 38°S a 43°S, Cordillera de la Costa, Chile. *In*: *8th Congreso Geológico Chileno*, *Antofagasta, Actas I*, 98–102.

Kato, T.T., Sharp, W. & Godoy, E. 2008. Inception of a Devonian subduction zone along the southwestern Gondwana margin: $^{40}Ar/^{39}Ar$ dating of eclogite–amphibolite assemblage in blueschist boulders from the coastal range of Chile 41°S. *Canadian Journal of Earth Sciences*, **45**, 337–351.

Levi, B., Aguilar, A. & Fuenzalida, R. 1966. *Reconocimiento geológico en las provincias Llanquihue y Chiloé. Instituto de Investigaciones Geológicas, Santiago, Boletín*, **19**.

Ludwig, K.R. 2003. *Isoplot 3.0, A Geochronological Toolkit for Microsoft Excel. Berkeley Geochronology Center, Special Publication*, **4**.

Ludwig, K.R. 2009. *SQUID 2: A User's Manual, rev. 12 Apr, 2009. Berkeley Geochronology Center, Special Publication*, **5**.

Maksymowicz, A. 2015. The geometry of the Chilean continental wedge: Tectonic segmentation of subduction processes off Chile. *Tectonophysics*, **659**, http://dx.doi.org/10.1016/j.tecto.2015.08.007.

Martin, M., Kato, T., Rodríguez, C., Godoy, E., Duhart, P., McDonough, M. & Campos, A. 1999. Evolution of late Paleozoic accretionary complex and overlying forearc–magmatic arc, South–Central Chile 38°–41°S: constraints for the tectonic setting along the southwestern margin of Gondwana. *Tectonics*, **18**, 582–605.

McDonough, M., Ugalde, H., Duhart, P. & Crignola, P. 1997. Nuevos antecendentes estructurales de la Cordillera de la Costa y el adyacente Valle Central en la parte norte de la Xa Región, Chile: su relación con el patrón magnético. *In*: *8th Congreso Geológico Chileno*, *Antofagasta, Actas I*, 169–172.

Miyashiro, A. 1961. Evolution of metamorphic belts. *Journal of Petrology*, **2**, 277–311.

Munizaga, F., Hervé, F., Drake, R., Pankhurst, R.J., Brook, M. & Snelling, N.J. 1988. Geochronology of the Lake Region of South–Central Chile 39°–42°S: preliminary results. *Journal of South American Earth Sciences*, **1**, 309–316.

Pankhurst, R.J., Hervé, F., Rojas, L. & Cembrano, J. 1992. Magmatism and tectonics in continental Chiloe, Chile 42–42°30'S. *Tectonophysics*, **205**, 283–294.

Pankhurst, R.J., Weaver, S.D., Hervé, F. & Larrondo, P. 1999. Mesozoic–Cenozoic evolution of the North Patagonian Batholith in Aysén, Southern Chile. *Journal of the Geological Society, London*, **156**, 673–694, http://dx.doi.org/10.1144/gsjgs.156.4.0673.

Pankhurst, R.J., Rapela, C.W., Fanning, C.M. & Márquez, M. 2006. Gondwanide continental collision and the origin of Patagonia. *Earth-Science Reviews*, **76**, 235–257.

Pankhurst, R.J., Rapela, C.W., López de Luchi, M.G., Rapalini, A.E., Fanning, C. M. & Galindo, C. 2014. The Gondwana connections of Patagonia. *Journal of the Geological Society, London*, **171**, 313–328, http://dx.doi.org/10.1144/jgs2013-081.

Quezada, P. 2015. *Geología del basamento de la Región de Los Lagos, Chile: evidencias de magmatismo calco alcalino y aportes sedimentarios devónicos*. Graduation thesis, Universidad de Chile, Santiago.

Ramos, V.A. Jordan, T.E., Allmendinger, R.W., Mpodozis, C., Kay, S.M., Cortes, J. & Palma, M. 1986. Paleozoic terranes of the Central Argentine Chilean Andes. *Tectonics*, **5**, 855–880.

Rapalini, A.E., López de Luchi, M., Tohver, E. & Cawood, P.A. 2013. The South American ancestry of the North Patagonian Massif: geochronological evidence for an autochthonous origin? *Terra Nova*, **25**, 337–342, http://dx.doi.org/10.1111/ter.12043.

Romero, R. 2014. *Proveniencia de Sedimentos en el Complejo Acrecionario Paleozoico entre 36°30'S y 40°S*. Graduation thesis, Universidad de Chile, Santiago.

Thiele, R., Hervé, F. & Parada, M.A. 1976. Bosquejo geológico de la Isla Huapi, Lago Ranco, Provincia de Valdivia. *In*: *1st Congreso Geológico Chileno*, *Santiago, Actas I*, A115–A132.

Tomezzoli, R.N. 2012. Chilenia y Patagonia: ¿un mismo continente a la deriva? *Revista de la Asociación Geológica Argentina*, **69**, 222–239.

Valley, J.W., Kinny, P.D., Schulze, D.J. & Spicuzza, M.J. 1998. Zircon megacrysts from kimberlite: oxygen-isotope variability among mantle melts. *Contributions to Mineralogy and Petrology*, **133**, 1–11.

Varela, R., Basei, M.A.S., Cingolani, C.A., Siga, O., Jr. & Passarelli, C.R. 2005. El basamento cristalino de los Andes norpatagónicos en Argentina: geocronología e interpretación tectónica. *Revista Geológica de Chile*, **32**, 167–182.

White, L.T. & Ireland, T.R. 2012. High-uranium matrix effect in zircon and its implications for SHRIMP U–Pb age determinations. *Chemical Geology*, **306–307**, 78–91.

Williams, I.S. & Hergt, J.M. 2000. U–Pb dating of Tasmanian dolerites: a cautionary tale of SHRIMP analysis of high-U zircon. *In*: Woodhead, J.D., Hergt, J.M. & Noble, W.P. (eds) *Beyond 2000: New Frontiers in Isotope Geoscience, Lorne, 2000; Abstracts and Proceedings*, Eastern Press, Mulgrave, Victoria, Australia, 185–188.

Willner, A.P., Thomson, S.N., Kröner, A., Wartho, J.A., Wijbrans, J. & Hervé, F. 2005. Time markers for the evolution and exhumation history of an Upper Paleozoic paired metamorphic belt in Central Chile 34°–35°30′S. *Journal of Petrology*, **46**, 1835–1858.